

A semiclassical study of the Jaynes-Cummings model.

O. Babelon, L. Cantini, B. Douçot.

8 May 2009

Laboratoire de Physique Théorique et Hautes Energies¹
Unité Mixte de Recherche UMR 7589
Université Pierre et Marie Curie-Paris6; CNRS;

Abstract. We consider the Jaynes-Cummings model of a single quantum spin s coupled to a harmonic oscillator in a parameter regime where the underlying classical dynamics exhibits an unstable equilibrium point. This state of the model is relevant to the physics of cold atom systems, in non-equilibrium situations obtained by fast sweeping through a Feshbach resonance. We show that in this integrable system with two degrees of freedom, for any initial condition close to the unstable point, the classical dynamics is controlled by a singularity of the focus-focus type. In particular, it displays the expected monodromy, which forbids the existence of global action-angle coordinates. Explicit calculations of the joint spectrum of conserved quantities reveal the monodromy at the quantum level, as a dislocation in the lattice of eigenvalues. We perform a detailed semi-classical analysis of the associated eigenstates. Whereas most of the levels are well described by the usual Bohr-Sommerfeld quantization rules, properly adapted to polar coordinates, we show how these rules are modified in the vicinity of the critical level. The spectral decomposition of the classically unstable state is computed, and is found to be dominated by the critical WKB states. This provides a useful tool to analyze the quantum dynamics starting from this particular state, which exhibits an aperiodic sequence of solitonic pulses with a rather well defined characteristic frequency.

1 Introduction.

The Jaynes-Cummings model was originally introduced to describe the near resonant interaction between a two-level atom and a quantized mode of the electromagnetic field [1]. When the field is treated classically, the populations of the two levels exhibit periodic Rabi oscillations whose frequency is proportional to the field intensity. The full quantum treatment shows that the possible oscillation frequencies are quantized, and are determined by the total photon number stored in the

¹ LPTHE, Tour 24-25, 5ème étage, Boîte 126, 4 Place Jussieu, 75252 Paris Cedex 05.

mode. For an initial coherent state of the field, residual quantum fluctuations in the photon number lead to a gradual blurring and a subsequent collapse of the Rabi oscillations after a finite time. On even longer time scales, the model predicts a revival of the oscillations, followed later by a second collapse, and so on. These collapses and revivals have been analyzed in detail by Narozhny et al [3], building on the exact solution of the Heisenberg equations of motion given by Ackerhalt and Rzazewski [2]. Such complex time evolution has been observed experimentally on the Rydberg micromaser [4]. More recently, a direct experimental evidence that the possible oscillation frequencies are quantized has been achieved with Rydberg atoms interacting with the small coherent fields stored in a cavity with a large quality factor [5]. Another interesting feature of the Jaynes-Cummings model is that it provides a way to prepare the field in a linear superposition of coherent states [6]. In the non resonant case, closely related ideas were used to measure experimentally the decoherence of Schrödinger cat states of the field in a cavity [7].

In the present paper, we shall consider the generalization of the Jaynes-Cummings model where the two-level atom is replaced by a single spin s . One motivation for this is the phenomenon of superradiance, where a population of identical two-level atoms interacts coherently with the quantized electromagnetic field. As shown by Dicke [8], this phenomenon can be viewed as the result of a cooperative behavior, where individual atomic dipoles build up to make a macroscopic effective spin. In the large s limit, and for most initial conditions, a semi-classical approach is quite reliable. However, the corresponding classical Hamiltonian system with two degrees of freedom is known to exhibit an unstable equilibrium point, for a large region in its parameter space. As shown by Bonifacio and Preparata [9], the subsequent evolution of the system, starting from such a state, is dominated by quantum fluctuations as it would be for a quantum pendulum initially prepared with the highest possible potential energy. These authors have found that, at short times, the evolution of the system is almost periodic, with solitonic pulses of photons separating quieter time intervals where most of the energy is stored in the macroscopic spin. Because the stationary states in the quantum system have eigenenergies that are not strictly equidistant, this quasiperiodic behavior gives way, at longer times, to a rather complicated pattern, that is reminiscent of the collapses and revivals in the $S = 1/2$ Jaynes-Cummings model.

An additional motivation for studying the large s Jaynes-Cummings model comes from recent developments in cold atom physics. It has been shown that the sign and the strength of the two body interaction can be tuned at will in the vicinity of a Feshbach resonance, and this has enabled various groups to explore the whole crossover from the Bose Einstein condensation of tightly bound molecules [10] to the BCS condensate of weakly bound atomic pairs [11, 12]. In the case of a fast sweeping of the external magnetic field through a Feshbach resonance, some coherent macroscopic oscillations in the molecular condensate population have been predicted theoretically [13], from a description of the low energy dynamics in terms of a collection of N spins $1/2$ coupled to a single harmonic oscillator. This model has been shown to be integrable [14] by Yuzbashyan et al. who emphasized its connection with the original integrable Gaudin model [15]. It turns out that in the cross-over region, the free Fermi sea is unstable towards the formation of a pair condensate, and that this instability is manifested by the appearance of two pairs of conjugated complex frequencies

in a linear analysis. This shows that for any value of N (which is also half of the total number of atoms), these coherent oscillations are well captured by an effective model with two degrees of freedom, one spin, and one oscillator. Therefore, there is a close connection between the quantum dynamics in the neighborhood of the classical unstable point of the Jaynes-Cummings model, and the evolution of a cold Fermi gas after an attractive interaction has been switched on suddenly.

The problem of quantizing a classical system in the vicinity of an unstable equilibrium point has been a subject of recent interest, specially in the mathematical community. The Bohr-Sommerfeld quantization principle suggests that the density of states exhibits, in the \hbar going to zero limit, some singularity at the energy of the classical equilibrium point, in close analogy to the Van Hove singularities for the energy spectrum of a quantum particle moving in a periodic potential. This intuitive expectation has been confirmed by rigorous [16, 17, 18] and numerical [19] studies. In particular, for a critical level of a system with one degree of freedom, there are typically $|\ln \hbar|$ eigenvalues in an energy interval of width proportional to \hbar around the critical value [17, 18]. A phase-space analysis of the corresponding wave-functions shows that they are concentrated along the classical unstable orbits which leave the critical point in the remote past and return to it in the remote future [16]. To find the eigenstates requires an extension of the usual Bohr-Sommerfeld rules, because matching the components of the wave-function which propagate towards the critical point or away from it is a special fully quantum problem, which can be solved by reduction to a normal form [16, 20].

Finally, we will show that the spin s Jaynes-Cummings model is an example of an integrable system for which it is impossible to define global action-angle coordinates. By the Arnold-Liouville theorem, classical integrability implies that phase space is foliated by n -dimensional invariant tori. Angle coordinates are introduced by constructing n -independent periodic Hamiltonian flows on these tori. Hence each invariant torus is equipped with a lattice of symplectic translations which act as the identity on this torus, the lattice of periods of these flows, which is equivalent to the data of n independent cycles on the torus. To get the angles we still must choose an origin on these cycles. All this can be done in a continuous way for close enough nearby tori showing the existence of local action angle variables. Globally, a first obstruction can come from the impossibility of choosing an origin on each torus in a consistent way. In the case of the Jaynes-Cummings model, this obstruction is absent (see [21], page 702). The second obstruction to the existence of global action-angle variables comes from the impossibility of choosing a basis of cycles on the tori in a uniform way. More precisely, along each curve in the manifold of regular invariant tori, the lattice associated to each torus can be followed by continuity. This adiabatic process, when carried along a closed loop, induces an automorphism on the lattice attached to initial (and final) torus, which is called the monodromy [21]. Several simple dynamical systems, including the spherical pendulum [21] or the champagne bottle potential [22] have been shown to exhibit such phenomenon. After quantization, classical monodromy induces topological defects such as dislocations in the lattice of common eigenvalues of the mutually commuting conserved operators [23]. Interesting applications have been found, specially in molecular physics [24]. In the Jaynes-Cummings model, the monodromy is directly associated to the unstable critical point, because it belongs to

a singular invariant manifold, namely a pinched torus. This implies that the set of regular tori is not simply connected, which allows for a non-trivial monodromy, of the so-called focus-focus type [25, 26, 27]. The quantization of a generic system which such singularity has been studied in detail by Vũ Ngọc [28]. Here, we present an explicit semi-classical analysis of the common energy and angular momentum eigenstates in the vicinity of their critical values, which illustrates all the concepts just mentioned.

In section [2] we introduce the classical Jaynes-Cummings model and describe its stationary points, stable and unstable. We then explain and compute the classical monodromy when we loop around the unstable point. We also introduce a reduced system that will be important in subsequent considerations. In section [3] we define the quantum model and explain that the appearance of a defect in the joint spectrum of the two commuting quantities is directly related to the monodromy phenomenon in the classical theory. In section [4] we perform the above reduction directly on the quantum system and study its Bohr-Sommerfeld quantization. The reduction procedure favors some natural coordinates which however introduce some subtleties in the semi classical quantization : there is a subprincipal symbol and moreover the integral of this subprincipal symbol on certain trajectories may have unexpected jumps. We explain this phenomenon. The result is that the Bohr-Sommerfeld quantization works very well everywhere, except for energies around the critical one. In section [5] we therefore turn to the semiclassical analysis of the system around the unstable stationary point. We derive the singular Bohr-Sommerfeld rules. Finally in section [6] we apply the previous results to the calculation of the time evolution of the molecule formation rate, starting from the unstable state. For this we need the decomposition of the unstable state on the eigenstates basis. We find that only a few states contribute and there is a drastic reduction of the dimensionality of the relevant Hilbert space. To compute these coefficients we remark that it is enough to solve the time dependent Schrödinger equation for small time. We perform this analysis and we show that we can extend it by gluing it to the time dependant WKB wave function. This gives new insights on the old result of Bonifacio and Preparata.

2 Classical One-spin system.

2.1 Stationary points and their stability

Hence, we consider the following Hamiltonian

$$H = 2\epsilon s^z + \omega \bar{b}b + g(\bar{b}s^- + bs^+) \quad (1)$$

Here $s^z = s^3$, $s^\pm = s^1 \pm is^2$ are spins variables, and b, \bar{b} is a harmonic oscillator. The Poisson brackets read

$$\{s^a, s^b\} = -\epsilon_{abc}s^c, \quad \{b, \bar{b}\} = i \quad (2)$$

Changing the sign of g amounts to changing $(b, \bar{b}) \rightarrow (-b, -\bar{b})$ which is a symplectic transformation. Rescaling the time we can assume $g = 1$.

The Poisson bracket of the spin variables is degenerate. To obtain a symplectic manifold, we fix the value of the Casimir function

$$\vec{s} \cdot \vec{s} = (s^z)^2 + s^+ s^- = s_{cl}^2$$

so that the corresponding phase space becomes the product of a sphere by a plane and has a total dimension 4. Let us write

$$H = H_0 + \omega H_1$$

with

$$H_1 = \bar{b}b + s^z, \quad H_0 = 2\kappa s^z + \bar{b}s^- + bs^+, \quad \kappa = \epsilon - \omega/2 \quad (3)$$

Clearly we have

$$\{H_0, H_1\} = 0$$

so that the system is integrable¹. Hence we can solve simultaneously the evolution equations

$$\partial_{t_0} f = \{H_0, f\}, \quad \partial_{t_1} f = \{H_1, f\}$$

Once $f(t_0, t_1)$ is known, the solution of the equation of motion $\partial_t f = \{H, f\} = (\partial_{t_0} + \omega \partial_{t_1})f$ is given by $f(t, \omega t)$. The equations of motion read

$$\partial_{t_1} b = -ib \quad \partial_{t_0} b = -is^- \quad \partial_t b = -is^- - i\omega b \quad (4)$$

$$\partial_{t_1} s^z = 0 \quad \partial_{t_0} s^z = i(\bar{b}s^- - bs^+) \quad \partial_t s^z = i(\bar{b}s^- - bs^+) \quad (5)$$

$$\partial_{t_1} s^+ = is^+ \quad \partial_{t_0} s^+ = 2i\kappa s^+ - 2i\bar{b}s^z \quad \partial_t s^+ = 2i\epsilon s^+ - 2i\bar{b}s^z \quad (6)$$

$$\partial_{t_1} s^- = -is^- \quad \partial_{t_0} s^- = -2i\kappa s^- + 2ibs^z \quad \partial_t s^- = -2i\epsilon s^- + 2ibs^z \quad (7)$$

The t_1 evolution is simply a simultaneous rotation around the z axis of the spin and a rotation of the same angle of the harmonic oscillator part:

$$b(t_0, t_1) = e^{-it_1} b(t_0), \quad s^\pm(t_0, t_1) = e^{\pm it_1} s^\pm(t_0), \quad s^z(t_0, t_1) = s^z(t_0) \quad (8)$$

In physical terms, the conservation of H_1 corresponds to the conservation of the total number of particles in the system, when this model (with N quantum spins 1/2) is used to describe the coherent dynamics between a Fermi gas and a condensate of molecules [13].

We wrote the full equations of motion to emphasize the fact that the points

$$s^\pm = 0, \quad s^z = \pm s_{cl}, \quad b = b^\dagger = 0 \quad (9)$$

are *all* the critical points (or stationary points i.e. all time derivatives equal zero) of *both* time evolutions t_0 and t_1 and hence are very special. Any Hamiltonian, function of H_0 and H_1 , will have these two points among its critical points. However, it may have more.

¹This remains true for the N -spin system. In the Integrable Community this model is known to be a limiting case of the Gaudin model [14]

For instance when $H = H_0 + \omega H_1$ an additional family of stationary points exist when $\omega^2 \epsilon^2 < s_{cl}^2$. They are given by

$$s^\pm = \sqrt{s_{cl}^2 - \epsilon^2 \omega^2} e^{\pm i\varphi}, \quad s^z = -\epsilon\omega, \quad b = -\frac{1}{\omega} \sqrt{s_{cl}^2 - \epsilon^2 \omega^2} e^{-i\varphi} \quad \forall \varphi \quad (10)$$

their energy is given by

$$E' = -\frac{1}{\omega} (s_{cl}^2 + \omega^2 \epsilon^2)$$

The energies of the configurations Eq. (9) are

$$E = \pm 2\epsilon s_{cl}$$

so that

$$E - E' = \frac{1}{\omega} (s_{cl} \pm \epsilon\omega)^2 > 0$$

and we see that E' represents the degenerate ground states of H , breaking rotational invariance around the z axis.

We are mostly interested in the configurations Eq. (9). To fix ideas we assume $\epsilon < 0$ so that among these two configurations, the one with minimal energy is the spin up. It looks like being a minimum however it becomes unstable for some values of the parameters. To see it, we perform the analysis of the small fluctuations around this configuration. We assume that b, \bar{b}, s^\pm are first order and $s^z = s_{cl}e + \delta s^z$ where $e = \pm 1$ according to whether the spin is up or down. Then δs^z is determined by saying that the spin has length s_{cl}

$$\delta s^z = -\frac{e}{2s_{cl}} s^- s^+$$

This is of second order and is compatible with Eq. (5). The linearized equations of motion (with respect to H) are

$$\dot{b} = -i\omega b - i s^- \quad (11)$$

$$\dot{s}^- = -2i\epsilon s^- + 2i s_{cl} e b \quad (12)$$

and their complex conjugate. We look for eigenmodes in the form

$$b(t) = b(0)e^{-2iEt}, \quad s^- = s^-(0)e^{-2iEt}$$

We get from Eq. (12)

$$s^-(0) = -s_{cl} \frac{e}{E - \epsilon} b(0)$$

Inserting into Eq. (11), we obtain the self-consistency equation for E :

$$E = \frac{\omega}{2} - \frac{s_{cl}}{2} \frac{e}{E - \epsilon} \quad (13)$$

The discriminant of this second degree equation for E is $\kappa^2 - 2s_{cl}e$. If $e = -1$ it is positive and we have a local energy maximum. However if $e = +1$, the roots become complex when $\kappa^2 \leq 2s_{cl}$. In that case one of the modes exponentially increases with time, i.e. the point is *unstable*. Since we are in a situation where $\kappa \leq 0$, the transition occurs when $\kappa = -\sqrt{2s_{cl}}$.

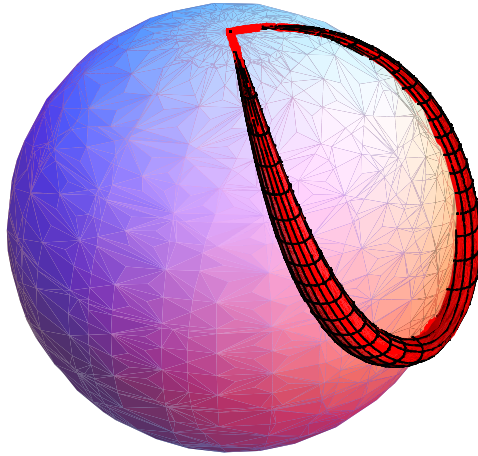


Figure 1: The image in phase space of the level set of the critical unstable point $H_0 = 2\kappa s_{cl}, H_1 = s_{cl}$ is a pinched two dimensional torus.

The level set of the unstable point, i.e. the set of points in the four-dimensional phase space of the spin-oscillator system, which have the same values of H_0 and H_1 as the critical point $H_0 = 2\kappa s_{cl}, H_1 = s_{cl}$ has the topology of a pinched two-dimensional torus see Fig.[1]. This type of stationary point is known in the mathematical litterature as a focus-focus singularity [25, 26, 27]. The above perturbation analysis shows that in the immediate vicinity of the critical point, the pinched torus has the shape of two cones that meet precisely at the critical point. One of these cones is associated to the unstable small perturbations, namely those which are exponentially amplified, whereas the other cone corresponds to perturbations which are exponentially attenuated. Of course, these two cones are connected, so that any initial condition located on the unstable cone gives rise

to a trajectory which reaches eventually the stable cone in a finite time. Note that this longitudinal motion from one cone to the other is superimposed to a spiraling motion around the closed cycle of the pinched torus which is generated by the action of H_1 .

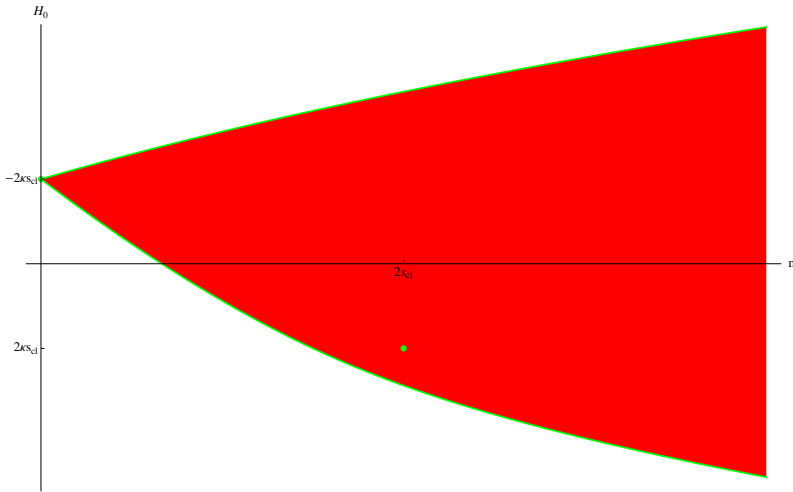


Figure 2: The image in R^2 of the phase space by the map $(H_1 \equiv m - s_{cl}, H_0)$. The green dots are the critical points. The stable one is the point on the vertical axis ($m = 0, -2\kappa s_{cl}$) and the unstable one is located at $(m = 2s_{cl}, 2\kappa s_{cl})$. The upper and lower green boundaries are obtained as explained in the text.

An important object is the image of phase space into R^2 under the map (H_1, H_0) . It is shown in Fig.[2]. It is a convex domain in R^2 . The upper and lower green boundaries are obtained as follows. We set $x = \bar{b}b$ and

$$H_1 = x + s^z \equiv m - s_{cl}, \quad \text{Max}(0, m - 2s_{cl}) \leq x \leq m \quad (14)$$

where the parameter m is introduced to ease the comparison with the quantum case. Then we set

$$b = \sqrt{x}e^{i\theta}, \bar{b} = \sqrt{x}e^{-i\theta}, \quad s^\pm = \sqrt{s_{cl}^2 - (s^z)^2}e^{\mp i\varphi} = \sqrt{(m-x)(2s_{cl}-m+x)}e^{\mp i\varphi}$$

so that

$$H_0 = 2\kappa(m - s_{cl} - x) + 2\sqrt{x(m-x)(2s_{cl}-m+x)} \cos(\theta - \varphi)$$

It follows that

$$2\kappa(m - s_{cl} - x) - 2\sqrt{x(m-x)(2s_{cl}-m+x)} \leq H_0 \leq 2\kappa(m - s_{cl} - x) + 2\sqrt{x(m-x)(2s_{cl}-m+x)}$$

To find the green curves in Fig.[2] we have to minimize the left hand side and maximize the right hand side in the above inequalities when x varies in the bounds given in Eq. (14).

In the unstable case, because an initial condition close to the critical point leads to a large trajectory along the pinched torus, it is interesting to know the complete solutions of the equations of motion. They are easily obtained as follows. Remark that

$$\begin{aligned} (\dot{s}^z)^2 &= -(\bar{b}s^- - bs^+)^2 = -(\bar{b}s^- + bs^+)^2 + 4\bar{b}bs^+s^- \\ &= -(H_0 - 2\kappa s^z)^2 + 4(H_1 - s^z)(s_{cl}^2 - (s^z)^2) \end{aligned}$$

or

$$(\dot{s}^z)^2 = 4(s^z)^3 - 4(H_1 + \kappa^2)(s^z)^2 + 4(\kappa H_0 - s_{cl}^2)s^z + (4s_{cl}^2 H_1 - H_0^2)$$

Hence, s^z satisfies an equation of the Weierstrass type and is solved by elliptic functions. Indeed, setting

$$s^z = \frac{1}{3}(H_1 + \kappa^2) - X, \quad \dot{s}^z = iY$$

the equation becomes

$$Y^2 = 4X^3 - g_2X - g_3 \tag{15}$$

with

$$g_2 = \frac{4}{3}(H_1^2 - 3H_0\kappa + 2H_1\kappa^2 + \kappa^4 + 3s_{cl}^2)$$

$$g_3 = \frac{1}{27}(-27H_0^2 - 8H_1^3 + 36H_0H_1\kappa - 24H_1^2\kappa^2 + 36H_0\kappa^3 - 24H_1\kappa^4 - 8\kappa^6 + 72H_1s_{cl}^2 - 36\kappa^2s_{cl}^2)$$

Therefore, the general solution of the one-spin system reads

$$s^z = \frac{1}{3}(H_1 + \kappa^2) - \wp(it + \alpha) \tag{16}$$

and

$$\bar{b}b = H_1 - s^z = \frac{1}{3}(2H_1 - \kappa^2) + \wp(it + \alpha) \tag{17}$$

where α is an integration constant and $\wp(\theta)$ is the Weierstrass function associated to the curve Eq. (15). Initial conditions can be chosen such that when $t = 0$, we start from a point intersecting the real axis $Y = 0$. This happens when α is half a period:

$$\alpha = \omega_1 \text{ or } \omega_2 \text{ or } \omega_3 = -\omega_1 - \omega_2$$

This general solution however is not very useful because the physics we are interested in lies on Liouville tori specified by very particular values of the conserved quantities H_0, H_1 . For the configuration Eq. (9) with spin up, the values of the Hamiltonians are

$$H_0 = 2\kappa s_{cl}, \quad H_1 = s_{cl}$$

In that case we have

$$g_2 = \frac{4}{3}\Omega^4, \quad g_3 = \frac{8}{27}\Omega^6$$

and

$$4X^3 - g_2X - g_3 = 4 \left(X + \frac{1}{3}\Omega^4 \right)^2 \left(X - \frac{2}{3}\Omega^2 \right)$$

where we have defined

$$\Omega^2 = 2s_{cl} - \kappa^2 > 0 \text{ in the } \textit{unstable} \text{ case.} \quad (18)$$

Hence, we are precisely in the case where the elliptic curve degenerates. Then the solution of the equations of motion is expressed in terms of trigonometric functions

$$X(t) = \frac{2}{3}\Omega^2 - \Omega^2 \tanh^2(\Omega(t - t_0))$$

and

$$x(t) \equiv \bar{b}b(t) = \frac{\Omega^2}{\cosh^2 \Omega(t - t_0)} \quad (19)$$

This solution represents a single solitonic pulse centered at time t_0 . When the initial condition is close but not identical to the unstable configuration with spin up and $b = \bar{b} = 0$, this unique soliton is replaced by a periodic sequence of pulses that can be described in terms of the Weierstrass function as shown above. Note that in the context of cold fermionic atoms, $\bar{b}b$ represents the number of molecular bound-states that have been formed in the system.

2.2 Normal form and monodromy

The dynamics in the vicinity of the unstable equilibrium can also be visualized by an appropriate choice of canonical variables in which the quadratic parts in the expansions of H_0 and H_1 take a simple form. Let us introduce the angle $\nu \in]0, \pi/2[$ such that $|\kappa| = \sqrt{2s_{cl}} \cos \nu$ and $\Omega = \sqrt{2s_{cl}} \sin \nu$. As we have shown, instability occurs when $\kappa^2 < 2s_{cl}$, which guarantees that ν is real. Let us then define two complex coordinates A_s and A_u by:

$$\begin{pmatrix} A_s \\ A_u \end{pmatrix} = \frac{1}{\sqrt{2 \sin \nu}} \begin{pmatrix} e^{-i\nu/2} & e^{i\nu/2} \\ e^{i\nu/2} & e^{-i\nu/2} \end{pmatrix} \begin{pmatrix} b \\ \frac{s^-}{\sqrt{2s_{cl}}} \end{pmatrix} \quad (20)$$

The classical Poisson brackets for these variables are:

$$\{A_s, \bar{A}_s\} = \{A_u, \bar{A}_u\} = 0 \quad (21)$$

$$\{A_s, \bar{A}_u\} = \{\bar{A}_s, A_u\} = 1 \quad (22)$$

Here we have approximated the exact relation $\{s^+, s^-\} = 2is^z$ by $\{s^+, s^-\} = 2is_{cl}$, which is appropriate to capture the linearized flow near the unstable fixed point. After subtracting their

values at the critical point which do not influence the dynamics, the corresponding quadratic Hamiltonian H_0 and global rotation generator H_1 read:

$$H_0 = 2\Omega\Re(\bar{A}_s A_u) + \kappa H_1 \quad (23)$$

$$H_1 = 2\Im(\bar{A}_s A_u) \quad (24)$$

With the above Poisson brackets, the linearized equations of motion take the form:

$$\dot{A}_s = (-\Omega - i\kappa)A_s \quad (25)$$

$$\dot{A}_u = (\Omega - i\kappa)A_u \quad (26)$$

With these new variables, the pinched torus appears, in the neighborhood of the unstable point, as the union of two planes intersecting transversally. These are defined by $A_u = 0$ which corresponds to the stable branch, and by $A_s = 0$ which gives the unstable branch. The global rotations generated by H_1 multiply both A_s and A_u by the same phase factor e^{-it_1} . We may then visualize these two planes as two cones whose common tip is the critical point, as depicted on Fig. 1. The stable cone is obtained from the half line where A_s is real and positive and $A_u = 0$, after the action of all possible global rotations. A similar description holds for the unstable cone. As shown by Eq. (19), any trajectory starting from the unstable branch eventually reaches the stable one. This important property will play a crucial role below in the computation of the monodromy.

For latter applications, specially in the quantum case, it is useful to write down explicitly A_s and A_u in terms of their real and imaginary parts:

$$A_s = (P_1 - iP_2)/\sqrt{2} \quad (27)$$

$$A_u = (X_1 - iX_2)/\sqrt{2} \quad (28)$$

This reproduces the above Poisson brackets, provided we set $\{X_i, X_j\} = 0$, $\{P_i, P_j\} = 0$, $\{P_i, X_j\} = \delta_{ij}$ for $i, j \in \{1, 2\}$. The quadratic Hamiltonian now reads:

$$H_0 = \Omega(X_1 P_1 + X_2 P_2) + \kappa H_1 \quad (29)$$

$$H_1 = X_1 P_2 - X_2 P_1 \quad (30)$$

which is the standard normal form for the focus-focus singularity [25, 26, 27].

We are now in a position to define and compute the monodromy attached to a closed path around the unstable point in the (H_0, H_1) plane as in Fig. 2. Let us consider a one parameter family of regular invariant tori which are close to the pinched torus. This family can be described by a curve in the (H_0, H_1) plane, or equivalently, in the complex plane of the $\bar{A}_s A_u$ variable. Let us specialize to the case of a closed loop. Its winding number around the critical value in the (H_0, H_1) plane is the same as the winding number of $\bar{A}_s A_u$ around the origin in the complex plane. Let us consider now the path $\chi \in [0, 2\pi] \rightarrow \bar{A}_s A_u = \eta^2 e^{i\chi}$ where $\eta > 0$ is assumed to be small. To construct the monodromy, we need to define, for each value of χ , two vector fields on the

corresponding torus, which are generated by χ -dependent linear combinations of H_0 and H_1 and whose flows are 2π -periodic. Furthermore we require that the periodic orbits of these two flows generate a cycle basis (e_1, e_2) in the two-dimensional homology of the torus. This basis evolves continuously as χ increases from 0 to 2π . The monodromy expresses the fact that (e_1, e_2) can turn into a different basis after one closed loop in the (H_0, H_1) plane. The discussion to follow has been to a large extent inspired by Cushman and Duistermaat [27].

One of these two flows can be chosen as the 2π global rotation generated by H_1 . The corresponding orbits are circles which provide the first basic cycle e_1 . For the other one, we first emphasize that the flow generated by H_0 is not periodic in general. So, to get the other basic cycle e_2 , we have to consider the flow generated by an appropriate linear combination of H_0 and H_1 . To construct it, it is convenient to consider an initial condition $(A_s(0), A_u(0))$ such that $\bar{A}_s(0)A_u(0) = \eta^2 e^{i\chi}$ and $|A_s(0)| \ll |A_u(0)|$, that is close to the unstable manifold of the pinched torus. Let us pick a small enough $\zeta > 0$ so that the linearized equations of motion are still accurate when $|A_s(0)|^2 + |A_u(0)|^2 < \zeta^2$, and let us also assume that $\eta \ll \zeta$. Using the global rotation invariance of the dynamics, we may choose $A_u(0) = \zeta$ and $A_s(0) = \frac{\eta^2}{\zeta} e^{-i\chi}$. If we let the system evolve starting from this initial condition, $|A_s|$ will first decrease and $|A_u|$ will increase, so the trajectory becomes closer to the unstable torus, along its unstable manifold. After a finite time t_1 , the trajectory reappears in the neighborhood of the unstable fixed point, but now, near the stable manifold. This behavior can be seen either as a consequence of Eq. (19) for the trajectories on the pinched torus and extended to nearby trajectories by a continuity argument, or can be checked directly from the explicit solution of the classical dynamics Eqs. (16,17) in terms of the Weierstrass function. We may thus choose t_1 such that $|A_s(t_1)| = \zeta$. A very important property of $A_s(t_1)$ is that it has a well defined limit when η goes to zero, because in this limit, one recovers the trajectory on the pinched torus such that $A_s(0) = 0$ and $A_u(0) = \zeta$. As a result, when η is small enough, the argument of $A_s(t_1)$ in polar coordinates weakly depends on χ and the winding number of $A_s(t_1)$ when χ goes from 0 to 2π vanishes. We then let the system evolves until time t_2 using the linearized flow. The time t_2 is chosen in order to recover $|A_u(t_2)| = \zeta$. Using Eq. (26) and the fact that $\bar{A}_s A_u$ is conserved, this gives $t_2 - t_1 = (2/\Omega) \ln(\zeta/\eta)$. Furthermore, from $\bar{A}_s(t_1)A_u(t_1) = \eta^2 e^{i\chi}$ and Eq. (26), we deduce:

$$A_u(t_2) = e^{i\chi} \exp\left(-2i\frac{\kappa}{\Omega} \ln \frac{\zeta}{\eta}\right) A_s(t_1) \quad (31)$$

In general, we have no reason to expect that $A_u(t_2)$ should be equal to $A_u(0)$ so, to get a periodic flow on the torus, the evolution generated by H_0 during the time t_2 has to be followed by a global rotation of angle $\beta(\chi)$ given by:

$$e^{i\beta(\chi)} = e^{i\chi} \exp\left(-2i\frac{\kappa}{\Omega} \ln \frac{\zeta}{\eta}\right) A_s(t_1)/\zeta \quad (32)$$

The sign of β reflects the fact that the H_1 flow applied during the time β multiplies A_s and A_u by $e^{-i\beta}$. Note that because the flows associated to H_0 and H_1 commute, the composition of the

H_0 -flow during time t_2 and of the H_1 flow along an angle β can also be viewed as the flow generated by the linear combination $H_0 + (\beta/t_2)H_1$ during time t_2 . We have established the periodicity of this flow for the orbit starting from $A_u(0) = \zeta$ and $A_s(0) = \frac{\eta^2}{\zeta}e^{-i\chi}$. But any other orbit on the invariant torus characterized by $\bar{A}_s A_u = \eta^2 e^{i\chi}$ can be deduced from this one by a global rotation, which commutes with the flow of $H_0 + (\beta/t_2)H_1$. This establishes the periodicity of this latter flow, and therefore allows us to construct the other basic cycle $e_2(\chi)$, which depends smoothly on χ .

Because the winding number of $A_s(t_1)$ vanishes provided η is small enough, we have the crucial relation:

$$\beta(2\pi) = \beta(0) + 2\pi \quad (33)$$

In other words, when we follow by continuity the periodic flow generated by $H_0 + (\beta/t_2)H_1$ during time t_2 , the final flow is deduced from the initial one by a global rotation of 2π . To summarize, as χ increases smoothly from 0 to 2π , e_1 is left unchanged, whereas e_2 evolves into $e_2 + e_1$. In this basis, the monodromy matrix of the focus-focus singularity is then:

$$M = \begin{pmatrix} 1 & 1 \\ 0 & 1 \end{pmatrix} \quad (34)$$

2.3 Reduced system.

As we have discussed before, the common level set of H_0 and H_1 which contains the unstable critical point is a pinched torus. Since we are mostly interested in the time evolution of the oscillator energy $\bar{b}b$, and because this quantity is invariant under the Hamiltonian action of H_1 , it is natural to reduce the dynamics to the orbits of H_1 . For an initial condition on the pinched torus, this amounts to discard the spiraling motion around the torus, and to concentrate on the longitudinal motion from the stable cone to the unstable one. In other words, this reduction procedure reduces the pinched torus into a curve which has a cusp at the critical point. This is illustrated by the thick curve on Fig. 3.

An other description of this trajectory is given by the thick curve on Fig. 4 that will be discussed below. In practice, the first thing to do to implement this reduction is to fix the value of H_1 to its critical value

$$H_1 = \bar{b}b + s^z = s_{cl} \quad (35)$$

This defines a submanifold $\mathcal{H}_{s_{cl}}$ in phase space. Since H_0 and H_1 Poisson commute we may consider the reduced system obtained by performing a Hamiltonian reduction by the one parameter group generated by H_1 . The reduced phase space is the quotient of $\mathcal{H}_{s_{cl}}$ by the flow generated by H_1 (the trivial t_1 phases in Eq. (8)). It is of dimension 2. Explicitly, we set:

$$x = \bar{b}b > 0 \implies b = \sqrt{x}e^{i\theta}, \quad \bar{b} = \sqrt{x}e^{-i\theta}$$

From Eq. (35) and from the condition $(s^z)^2 + s^+ s^- = s_{cl}^2$ we deduce

$$s^z = s_{cl} - x, \quad \text{and} \quad s^\pm = \sqrt{x(2s_{cl} - x)}e^{\mp i\varphi} \quad (36)$$

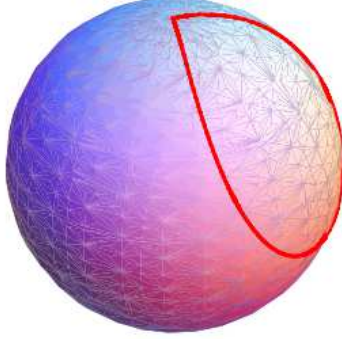


Figure 3: The sphere represents the reduced phase-space obtained by fixing the conserved quantity H_1 to its value s_{cl} at the critical point. Here, this point corresponds to the north pole on the sphere. The red curve is the image of the pinched torus after the reduction procedure. It is obtained by setting the other integral of motion H_0 to its critical value $H_0 = 2\kappa s_{cl}$. For this, we have used the expression of H_0 given in Eq. (37). The singular nature of the pinched torus is reflected by the cusp of the red curve at the north pole.

the reduced Hamiltonian H_0 reads

$$H_0 = 2\kappa s_{cl} + 2x\sqrt{2s_{cl} - x} \cos(\theta - \varphi) - 2\kappa x \quad (37)$$

Notice that x and $\theta - \varphi$ are invariant by the H_1 flow, and they can be taken as coordinates on the reduced phase space. These coordinates are canonically conjugate as we easily see by writing the symplectic form:

$$\omega = -i\delta b \wedge \delta \bar{b} + i\frac{\delta s^+}{s^+} \wedge \delta s^- = \delta x \wedge \delta(\theta - \varphi)$$

In the following, when talking about this reduced system, we will simply set $\varphi = 0$. These coordinates are very convenient but one has to be aware that they are singular at $x = 0$ and $x = 2s_{cl}$. The whole segment $x = 0, 0 \leq \theta < 2\pi$ should be identified to one point and similarly for the segment $x = 2s_{cl}, 0 \leq \theta < 2\pi$.

The equations of motion of the reduced system read

$$\begin{aligned} \dot{x} &= 2x\sqrt{2s_{cl} - x} \sin \theta \\ \dot{\theta} &= -2\kappa + 2 \left(\sqrt{2s_{cl} - x} - \frac{x}{2\sqrt{2s_{cl} - x}} \right) \cos \theta \end{aligned}$$

From this we see that the critical points are given by

$$x = 0, \quad \cos \theta = \frac{\kappa}{\sqrt{2s_{cl}}}, \quad \text{or} \quad z^2 - \frac{2\kappa}{\sqrt{2s_{cl}}}z + 1 = 0, \quad z = e^{i\theta}$$

In our case κ is negative, so that the solutions of the quadratic equations will be defined as

$$z_{\pm} = \frac{\kappa \pm i\Omega}{\sqrt{2s_{cl}}} = -e^{\mp i\nu}, \quad \Omega^2 = 2s_{cl} - \kappa^2, \quad 0 \leq \nu \leq \pi/2$$

These points exist precisely in the unstable regime $\kappa^2 \leq 2s_{cl}$. They correspond to only one point in phase space whose energy is given by

$$H_0 = 2\kappa s_{cl} \equiv E_c \tag{38}$$

hence they correspond to the unstable point. The image of the pinched critical torus after the reduction procedure is shown on Fig. 4 as the thick line connecting z_+ and z_- . Note that this line intersects the $x = 0$ segment with a finite angle. This angle reflects precisely the pinching of the torus at the unstable critical point in the original four-dimensional phase space.

Another critical point is obtained by setting $\theta = \pi$. Then

$$x = 2s_{cl} - X^2, \quad \text{with} \quad X = \frac{1}{3}(-\kappa + \sqrt{\kappa^2 + 6s_{cl}}) \tag{39}$$

Since $0 \leq x \leq 2s_{cl}$, we should also have $0 \leq X^2 \leq 2s_{cl}$ which is the case when $\kappa \geq -\sqrt{2s_{cl}}$, that is to say in the unstable region. The energy is given by

$$H_0 = 2\kappa s_{cl} - 2(X + \kappa)(2s_{cl} - X^2) \tag{40}$$

We see from that equation that, in the unstable region, $H_0 - 2\kappa s_{cl}$ is always negative and the configuration Eq. (39) represents the ground state.

Finally, the energy maximum of this reduced system is obtained for $\theta = 0$ and $x = 2s_{cl} - Y^2$, with $Y = (\kappa + \sqrt{\kappa^2 + 6})/3$. On the phase portrait shown on Fig. 4, one sees a curve which contains the point at $x = 2s_{cl}$ and which looks like a separatrix. However, unlike the situation around $x = 0$, we notice that it does not correspond to any stationary point of the unreduced Hamiltonian. In fact it is simple to show that the curve is actually tangent to the vertical line $x = 2s_{cl}$. On the sphere, this is the trajectory passing through the south pole.

3 Quantum One-spin system.

3.1 Energy spectrum

We now consider the quantum system. We set as in the classical case

$$H = H_0 + \omega H_1$$

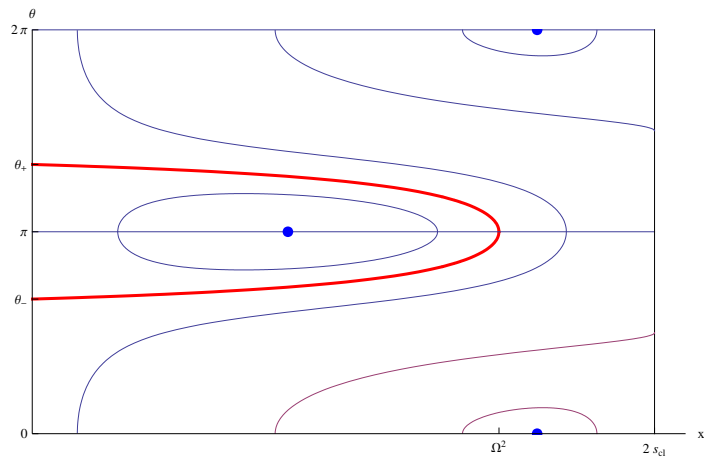


Figure 4: The phase portrait corresponding to the Hamiltonian H_0 , Eq. (37), in the (θ, x) variables, which are natural coordinates for the reduced system. The thick red line corresponds to the critical separatrix $H_0 = 2\kappa s_{cl}$, which is the image of the pinched critical torus after symplectic reduction. Note that the unstable critical point is mapped onto the vertical axis at $x = 0$, so that the critical separatrix is indeed a loop. The blue dots correspond to the minimal and maximal values of H_0 when $H_1 = s_{cl}$.

with

$$H_0 = (2\epsilon - \omega)s^z + b^\dagger s^- + bs^+ = 2\kappa s^z + b^\dagger s^- + bs^+, \quad H_1 = b^\dagger b + s^z$$

where as before

$$\kappa = \epsilon - \omega/2 \tag{41}$$

We impose the commutation relations

$$[b, b^\dagger] = \hbar, \quad [s^+, s^-] = 2\hbar s^z, \quad [s^z, s^\pm] = \pm\hbar s^\pm$$

We assume that the spin acts on a spin- s representation.

$$s^z|m\rangle = \hbar m|m\rangle, \quad s^\pm|m\rangle = \hbar\sqrt{s(s+1) - m(m\pm 1)}|m\pm 1\rangle, \quad m = -s, -s+1, \dots, s-1, s$$

where $2s$ is integer. Of course

$$(s^z)^2 + \frac{1}{2}(s^+s^- + s^-s^+) = \hbar^2 s(s+1)$$

We still have

$$[H_0, H_1] = 0$$

and the quantum system is integrable. The Hamiltonian H can be diagonalized by Bethe Ansatz, but we will not follow this path here. For related studies along this line for the Neumann model see [29]. Note that recently, the non equilibrium dynamics of a similar quantum integrable model (the Richardson model) has been studied by a combination of analytical and numerical tools. [30] Let:

$$e_n = (2b^\dagger)^n|0\rangle \otimes (s^+)^{M-n}| -s\rangle, \quad \text{Sup}(0, M-2s) \leq n \leq M \tag{42}$$

For all these states one has:

$$H_1 e_n = \hbar(M-s)e_n$$

Since H_0 commutes with H_1 we can restrict H_0 to the subspace spanned by the e_n . Hence, we write:

$$\Psi = \sum_{n=\text{Sup}(0, M-2s)}^M p_n \frac{e_n}{\|e_n\|},$$

where the norm $\|e_n\|$ of the vector e_n is given by:

$$\|e_n\|^2 = \hbar^{2M-n} 2^{2n} \frac{(2s)!(M-n)!n!}{(2s-M+n)!}$$

Using

$$H_0 e_n = 2\hbar\kappa(M-s-n)e_n + \frac{\hbar^2}{2}(M-n)(2s+1-M+n)e_{n+1} + 2\hbar n e_{n-1}$$

the Schrödinger equation

$$i\hbar \frac{\partial \Psi}{\partial t} = H_0 \Psi$$

becomes:

$$i\hbar \frac{\partial p_n}{\partial t} = \hbar^{\frac{3}{2}} \sqrt{(n+1)(2s+1-M+n)(M-n)} p_{n+1} + \hbar^{\frac{3}{2}} \sqrt{n(2s-M+n)(M+1-n)} p_{n-1} + 2\hbar\kappa(M-n-s)p_n$$

and the eigenvector equation $H_0 \Psi = E \Psi$ reads:

$$\begin{aligned} \hbar^{\frac{3}{2}} \sqrt{(n+1)(2s+1-M+n)(M-n)} p_{n+1} + \hbar^{\frac{3}{2}} \sqrt{n(2s-M+n)(M+1-n)} p_{n-1} & \quad (43) \\ + 2\hbar\kappa(M-n-s)p_n = E p_n & \quad (44) \end{aligned}$$

In this basis, the Hamiltonian is represented by a symmetric Jacobi matrix and it is easy to diagonalize it numerically. Varying $M = 0, 1, \dots$ we construct the lattice of the joint spectrum of H_0, H_1 . We see on Fig. 5 that the lattice has a defect located near the unstable classical point. This defect induces a quantum monodromy when we transport a cell of the lattice around it. The rule to transport a cell is as follows. We start with a cell and we choose the next cell in one of the four possible positions (east, west, north, south) in such a way that two edges of the new cell prolongate two sides of the original cell, and the two cells have a common edge. We apply these rules on a path which closes. If the path encloses the unstable point, the last cell is different from the initial cell.

The precise form of this lattice defect can be related to the classical monodromy matrix M , as shown by Vũ Ngọc [23]. Choosing locally a cycle basis e_i on the Arnold-Liouville tori is equivalent to specifying local action-angle coordinates (J_i, ϕ_i) such that e_i is obtained from the periodic orbit generated by J_i . After one closed circuit in the base space of this fibration by tori, the basic cycles are changed into $e'_i = \sum_j M_{ji} e_j$ and therefore, the new local action variables J'_i are deduced from the initial ones by:

$$J'_i = \sum_{j=1}^n M_{ji} J_j \quad (45)$$

Heuristically, the Bohr-Sommerfeld quantization principle may be viewed as the requirement that the quantum wave functions should be 2π periodic in each of the n phase variables ϕ_i , which implies that J_i should be an integer multiple of \hbar . When \hbar is small, the discrete set of common eigenvalues of the conserved operators has locally the appearance of a regular lattice, whose basis vectors v_1, \dots, v_n are approximately given by: $dJ_i(v_j) = \hbar \delta_{ij}$. Because of the monodromy, this lattice undergoes a smooth deformation as one moves around a critical value of the mutually commuting conserved quantities. After one complete turn, the basic lattice vectors are changed into v'_1, \dots, v'_n , which are also approximately given by: $dJ'_i(v'_j) = \hbar \delta_{ij}$. Taking into account the definition of the

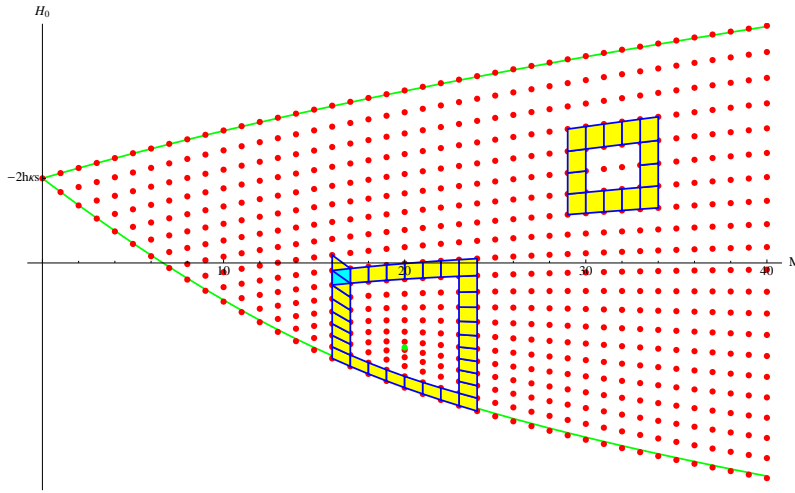


Figure 5: The lattice of the joint spectrum of H_0 and H_1 (or equivalently the integer M) in the unstable regime. The green point represents the classical unstable point ($H_1 = s_{cl}$, or $M = 2s$, and $H_0 = 2\kappa s_{cl}$). The parameters are $\hbar^{-1} = s = 10$, and $\kappa = -0.5\sqrt{2s_{cl}}$. This figure demonstrates the non-trivial quantum monodromy in this system. For this purpose, we follow by continuity an elementary cell of this lattice along two closed paths. When the path encloses the image of the critical point in the (H_0, H_1) plane, we see that an initial square cell does not preserve its shape at the end of the cycle, but it evolves into a parallelogram with a tilt. In other words, the lattice of joint eigenvalues exhibits a dislocation located at the critical value of H_0 and H_1 .

classical monodromy matrix in Eq (45), this leads to the semi-classical monodromy on the joint spectrum:

$$v'_i = \sum_{j=1}^n (M^{-1})_{ij} v_j \quad (46)$$

The discussion above was performed in the action angle variables (J_1, J_2) . In the (H_0, H_1) variables the basis v, v' should be transformed by the Jacobian matrix of the mapping $(J_1, J_2) \rightarrow (H_0(J_1, J_2), H_1(J_1, J_2))$.

On Fig. 5, we see that after a clockwise turn around the singular value in the (H_1, H_0) plane (which corresponds to a positive winding in the (H_0, H_1) plane), the lattice vectors v_M and v_{H_0} are transformed into $v_M - v_{H_0}$ and v_{H_0} respectively. This is in perfect agreement with the classical monodromy matrix computed in section 2.2.

When $M = 2s$, i.e. when H_1 takes its critical value corresponding to the unstable point,

$$H_1 e_n = \hbar s e_n$$

the Schrödinger equation simplifies to:

$$i\hbar \frac{\partial p_n}{\partial t} = \hbar^{\frac{3}{2}}(n+1)\sqrt{(2s-n)}p_{n+1} + \hbar^{\frac{3}{2}}n\sqrt{(2s+1-n)}p_{n-1} + 2\hbar\kappa(s-n)p_n \quad (47)$$

Setting

$$x = \hbar n, \quad s_{cl} = \hbar s$$

this equation becomes:

$$i\hbar \frac{\partial p(x)}{\partial t} = (x + \hbar)\sqrt{(2s_{cl} - x)}p(x + \hbar) + x\sqrt{(2s_{cl} + \hbar - x)}p(x - \hbar) + 2\kappa(s_{cl} - x)p(x) \quad (48)$$

Introducing the shift operator

$$e^{i\theta} p(x) = p(x + \hbar)$$

this can be rewritten as:

$$i\hbar \frac{\partial p(x)}{\partial t} = \left[\sqrt{(2s_{cl} - x)}e^{i\theta} x + x e^{-i\theta} \sqrt{(2s_{cl} - x)} + 2\kappa(s_{cl} - x) \right] p(x) \quad (49)$$

and we recognize the quantum version of the classical reduced Hamiltonian Eq. (37), but with a very specific ordering of the operators.

The eigenvector equation $H_0\Psi = E\Psi$ reads:

$$\hbar^{\frac{3}{2}}(n+1)\sqrt{(2s-n)}p_{n+1} + \hbar^{\frac{3}{2}}n\sqrt{(2s+1-n)}p_{n-1} + (2\hbar\kappa(s-n) - E)p_n = 0 \quad (50)$$

The eigenvalues are shown in Figure 6 in the stable case and in the unstable case.

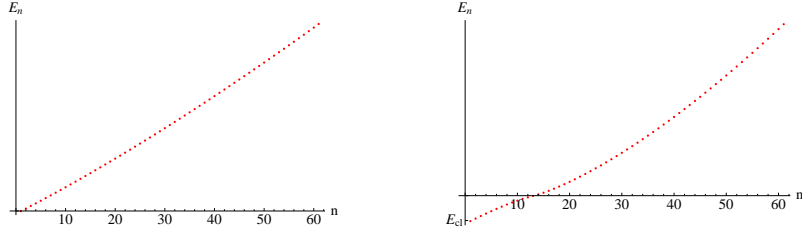


Figure 6: The eigenvalues of the reduced H_0 in the stable regime on the left and in the unstable case on the right. The origin of the Energy axis is the classical critical energy $E_c = 2\hbar s\kappa$. In the unstable case the ground state energy lies below this line and close to the classical value given by Eq. (40). ($\hbar^{-1} = s = 30$, $\kappa = -2\sqrt{2s_{cl}}$ (stable case), $\kappa = -0.5\sqrt{2s_{cl}}$ (unstable case)).

4 Bohr-Sommerfeld quantization

In this section we examine the standard semi-classical analysis of the one spin system. There are two complications as compared to the usual formulae. One comes from the fact that the phase space of the spin degrees of freedom is a 2-sphere and hence has a non trivial topology. The second one is related to the fact that the Schrödinger equation is a difference equation and its symbol has a subprincipal part. Let us recall the Schrödinger equation:

$$(x + \hbar)\sqrt{2s_{cl} - x} p(x + \hbar) + x\sqrt{2s_{cl} + \hbar - x} p(x - \hbar) - 2\kappa x p(x) = \hbar\epsilon p(x) \quad (51)$$

where

$$\hbar\epsilon = E - 2\hbar\kappa s, \quad x = \hbar n$$

The first thing to do is to compute the Weyl symbol $h(x, \theta)$ of the Hamiltonian operator. In standard notations, it is defined by:

$$(Hp)(x) = \frac{1}{2\pi\hbar} \int e^{-\frac{i}{\hbar}(x-y)\theta} h\left(\frac{x+y}{2}, \theta\right) p(y) d\theta dy$$

It is straightforward to check that, for the Hamiltonian of eq.(51)

$$h(x, \theta) = 2 \left(x + \frac{\hbar}{2}\right) \sqrt{2s_{cl} + \frac{\hbar}{2} - x} \cos \theta + 2\kappa(s_{cl} - x)$$

Expanding in \hbar we find the principal and sub-principal symbols

$$h(x, \theta) = h^0(x, \theta) + \hbar h^1(x, \theta) + \dots$$

where:

$$\begin{aligned} h^0(x, \theta) &= 2x\sqrt{2s_{cl} - x} \cos \theta + 2\kappa(s_{cl} - x) \\ h^1(x, \theta) &= \left(\sqrt{2s_{cl} - x} + \frac{x}{2\sqrt{2s_{cl} - x}} \right) \cos \theta \end{aligned}$$

We recognize, of course, that $h^0(x, \theta)$ is the classical Hamiltonian of the system Eq.(37). In particular the symplectic form reads:

$$\omega = dx \wedge d\theta$$

Note that the definition of the Weyl symbol we have used here is motivated by the simpler case where the classical phase space can be viewed as the cotangent bundle of a smooth manifold. In our case, the θ coordinate is 2π periodic, and we are not strictly speaking dealing with the cotangent bundle over the line parametrized by the x coordinate. To justify this procedure, we may first imbed our system in a larger phase space, where both θ and x run from $-\infty$ to ∞ . Because the symbol $h(x, \theta)$ is 2π periodic in θ , the unitary operator \mathcal{T} associated to the 2π translation of θ commutes with the quantum Hamiltonian H associated to the symbol $h(x, \theta)$. It is then possible to perform the semi-classical analysis in the enlarged Hilbert space and to project afterwards the states thus obtained on the subspace of 2π periodic wave-functions, which are eigenvectors of \mathcal{T} with the eigenvalue 1. Imposing the periodicity in θ forces x to be an integer multiple of \hbar . From Eq. (51), we see that the physical subspace, spanned by state vectors $|x = n\hbar\rangle$ with $0 \leq n \leq 2s$, is stable under the action of H .

An alternative approach would be to use a quantization scheme, such as Berezin-Toeplitz quantization [31], which allows to work directly with a compact classical phase-space such as the sphere. When H_1 takes its critical value corresponding to the unstable point, it is easy to show that the eigenvector equation (50) can be cast into the Schrödinger equation for a pure spin s Hamiltonian given by:

$$H_{\text{eff}} = 2\kappa s^z + s^+ \sqrt{s_{cl} - s_z} + \sqrt{s_{cl} - s_z} s^- \quad (52)$$

Starting from the known Toeplitz symbols of the basic spin operators, one may derive Bohr-Sommerfeld quantization rules directly from this Hamiltonian H_{eff} [32], but we shall not explore this further in this paper.

Returning to our main discussion we now choose a 1-form γ such that:

$$\gamma(X_{h^0}) = -h^1(x, \theta) \quad (53)$$

where X_{h^0} is the Hamiltonian vector field associated to the Hamiltonian $h^0(x, \theta)$, which is tangent to the variety $h^0(x, \theta) = E$. Using x as the coordinate on this manifold, we find:

$$X_{h^0} = 2x\sqrt{2s_{cl} - x} \sin \theta \partial_x$$

Hence, we may choose:

$$\gamma = -\frac{1}{2} \left(\frac{1}{x} + \frac{1}{2(2s_{cl} - x)} \right) \cot \theta dx$$

Under these circumstances, the Bohr-Sommerfeld quantization conditions involve the form γ and read (see e.g. [23])

$$\Phi_{Reg}(\epsilon) = \frac{1}{2\pi\hbar} \int_{C(E)} \alpha + \frac{1}{2\pi} \int_{C(E)} \gamma + \mu_{C(E)} \frac{1}{4} = n \quad (54)$$

where $C(E)$ is the classical trajectory of energy E , α is the canonical 1-form $\omega = d\alpha$, $\mu_{C(E)}$ is the Maslov index of this trajectory and n is an integer. Note that the integral of γ over $C(E)$ is completely specified by the constraint Eq.(53).

We now come to the fact that the 2-sphere has a non trivial topology. A consequence is that the canonical 1-form α does not exist globally. In the coordinates x, θ we may choose

$$\alpha = x d\theta$$

but this form is singular in the vicinity of the south pole where $x = 2s_{cl}$. Let us consider a closed path on the sphere parametrized by the segment at constant x , θ running from 0 to 2π . The integral of α around this path is $2\pi x$. When x goes to $2s_{cl}$, the integral goes to $4\pi s_{cl}$ which is the total area of the sphere. But the limit path for $x = 2s_{cl}$, corresponds on the sphere to a trivial loop, fixed at the south pole. The consistency of Bohr-Sommerfeld quantization requires then $4\pi s_{cl}$ to be an integer multiple of $2\pi\hbar$. Hence we recover the quantization condition of the spin: $2s$ should be an integer.

Before checking the validity of Eq.(54) in our system, it is quite instructive to plot the integral of γ along the curve $C(E)$ as a function of E . This is shown on Fig. 7 Here, we see two singularities at the values of E where $C(E)$ goes through either the north or the south pole. At the south pole $\int_{C(E)} \gamma$ merely jumps by π , whereas at the north pole, a jump of π is superimposed onto a logarithmic divergence. We can easily find an asymptotic formula for this integral for energies close to the critical value $E_c = 2s_{cl}\kappa$:

$$\oint \gamma = \frac{\kappa}{\Omega} \log \frac{\sqrt{2s_{cl}} |\Delta E|}{16\Omega^4} + 2(\pi - \nu) - \pi \Theta(\Delta E) + O(\Delta E, \Delta E \log |\Delta E|) \quad (55)$$

here $\Delta E = E - E_c$, and $\Theta(\Delta E) = 1$ if $\Delta E > 0$ and 0 if $\Delta E < 0$.

We wish now to show that these jumps are merely an effect of working with polar coordinates (x, θ) . It is instructive to consider first a quantum system with one degree of freedom, whose classical phase-space is the (q, p) plane. From any smooth function $h(p, q)$, we define the quantum operator $\mathcal{O}_{W,h}$ by:

$$(\mathcal{O}_{W,h}(\Psi))(q) = \frac{1}{2\pi\hbar} \int e^{\frac{i}{\hbar}(q-q')p} h\left(p, \frac{q+q'}{2}\right) \Psi(q') dp dq'$$

Polar coordinates are introduced, at the classical level by:

$$(p, q) = \sqrt{2x}(\cos \theta, \sin \theta)$$

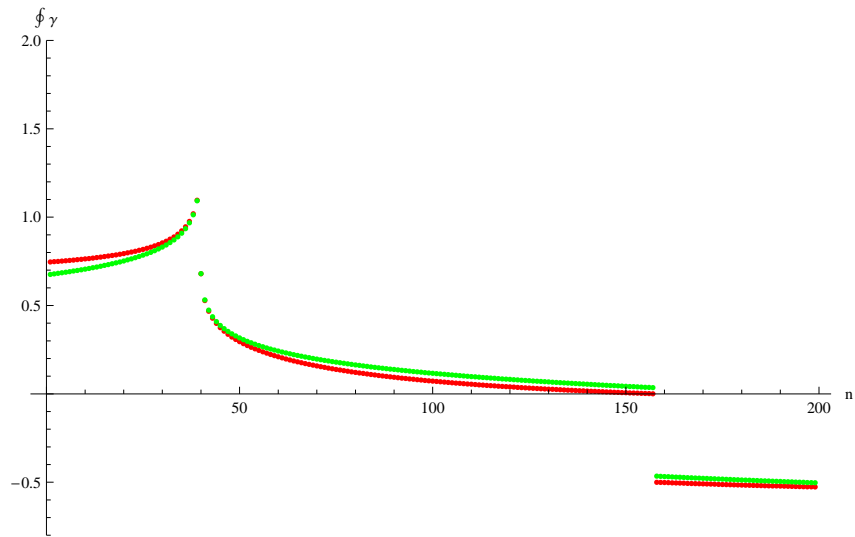


Figure 7: The integral of the sub-dominant symbol as a function of energy (the red curve). We see the logarithmic divergence for the energy corresponding to the singular critical point, and the gap $-\pi$ at the energy corresponding to the trajectory passing through the south pole. The green curve is the asymptotic formula Eq.(55) in which we have added the gap at the south pole to ease comparison and to show that it remains quite accurate even well beyond its expected range of validity.

This definition implies that $dp \wedge dq = dx \wedge d\theta$. At the quantum level, we start with the usual (\hat{p}, \hat{q}) operators. In the Hilbert space $L^2(q)$, we introduce the eigenvector basis $\{|n\rangle\}$ of $\hat{p}^2 + \hat{q}^2$, such that $(\hat{p}^2 + \hat{q}^2)|n\rangle = \hbar(2n+1)|n\rangle$. We may then set $\hat{x} = \sum_{n \geq 0} \hbar n |n\rangle \langle n|$. To define $\hat{\theta}$, such that $[\hat{\theta}, \hat{x}] = i\hbar$, it is natural to enlarge the Hilbert space, allowing n to take also negative integer values as well. Then we set $\exp(i\hat{\theta})|n\rangle = |n+1\rangle$. From $a|n\rangle = \sqrt{n}|n-1\rangle$ and $a^+|n\rangle = \sqrt{n+1}|n+1\rangle$, we see that, in the physical subspace $n \geq 0$, we have $a = \hbar^{-1/2} \exp(-i\hat{\theta}) \hat{x}^{1/2}$ and $a^+ = \hbar^{-1/2} \hat{x}^{1/2} \exp(i\hat{\theta})$. The Weyl symbols, in the (x, θ) variables, of these operators are $\hbar^{-1/2}(x + \hbar/2)^{1/2} \exp(\mp i\theta)$. Using $\hat{p} = (\hbar/2)^{1/2}(a + a^+)$ and $\hat{q} = (\hbar/2)^{1/2}i(a - a^+)$, we deduce that the Weyl symbols of \hat{p} and \hat{q} in the (x, θ) variables are respectively $\sqrt{2x + \hbar} \cos \theta$ and $\sqrt{2x + \hbar} \sin \theta$. So the Weyl symbol is not invariant under the non-linear change of coordinates from (p, q) to (x, θ) . For linear functions of p and q the symbol in (x, θ) , denoted by $h_{\text{pol}}(x, \theta)$ is obtained from $h(p, q)$ by substituting p and q by their classical expressions as functions of (x, θ) and then by shifting x into $x + \hbar/2$. Such a simple rule does not hold for more complicated functions $h(p, q)$. Nevertheless, one can show that the substitution of $x \rightarrow x + \hbar/2$ gives the symbol $h_{\text{pol}}(x, \theta)$ up to first order in \hbar . Practically, this means that:

$$h_{\text{pol}}(x, \theta) = h(\sqrt{2x + \hbar} \cos \theta, \sqrt{2x + \hbar} \sin \theta) \quad \text{mod } \mathcal{O}(\hbar^2)$$

or, more explicitly:

$$h_{\text{pol}}(x, \theta) = h(p, q) + \frac{\hbar}{4x} \left(p \frac{\partial h}{\partial p}(p, q) + q \frac{\partial h}{\partial q}(p, q) \right) + \mathcal{O}(\hbar^2)$$

where $(p, q) = \sqrt{2x}(\cos \theta, \sin \theta)$. This has the following important consequence: even if $h(p, q)$ has no subprincipal part (i.e. it does not depend on \hbar), $h_{\text{pol}}(x, \theta)$ does acquire a subprincipal part $h_{\text{pol}}^1(x, \theta)$. Now, along any classical trajectory associated to $h(p, q)$, we have:

$$p \frac{\partial h}{\partial p}(p, q) + q \frac{\partial h}{\partial q}(p, q) = p\dot{q} - q\dot{p} = 2x\dot{\theta},$$

so $h_{\text{pol}}^1(x, \theta) = \dot{\theta}/2$. This striking result implies that, when we work in polar coordinates, the γ form associated to $h_{\text{pol}}^1(x, \theta)$ may be chosen as $-d\theta/2$. This immediately explains why $\int_{C(E)} \gamma$ jumps by $-\pi$ when the $h(p, q) = E$ orbit crosses the origin of the polar coordinates, because then $\int_{C(E)} d\theta$ jumps from 0 to 2π , see Fig. 8. Note that, in general, we expect $h(p, q)$ to have also a subprincipal part $h^1(p, q)$. But this gives an additional term to $h_{\text{pol}}^1(x, \theta)$ which is deduced from $h^1(p, q)$ simply by the classical change of variables from (p, q) to (x, θ) . This term has no reason to display any singularity when the classical trajectory goes through the origin. Remark that around the south pole, if we set

$$x = 2s_{cl} - y, \quad p = \sqrt{2y} \cos \theta, \quad q = \sqrt{2y} \sin \theta$$

then we can expand

$$h_0 = -2s_{cl}(\kappa + s_{cl}) + \kappa \left(\left(p + \frac{\sqrt{2}s_{cl}}{\kappa} \right)^2 + q^2 \right)$$

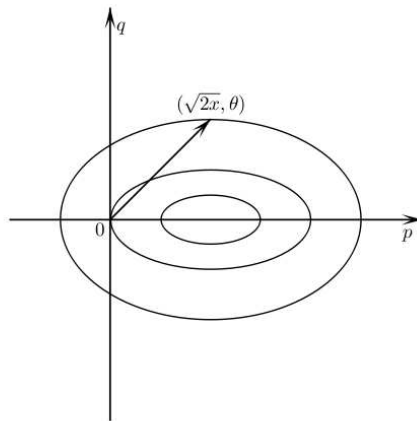


Figure 8: On this figure we see that $-\frac{1}{2} \oint d\theta$ equals zero if the integral is taken over the small ellipse, while it is equal to $-\pi$ if it is taken over the big ellipse enclosing the origin. This explains why the integral of the subprincipal symbol in polar coordinates jumps by $\pm\pi$ when the orbit crosses the origin of the polar coordinates.

and we see that our system is equivalent to a shifted harmonic oscillator.

Note that on the sphere, polar coordinates have two singularities, at the north and at the south poles, which correspond to $x = 0$ and $x = 2s_{cl}$ respectively. To generalize the above analysis to the sphere, we may thus use two charts (p, q) and (p', q') such that:

$$\begin{aligned} (p, q) &= \sqrt{2x}(\cos \theta, \sin \theta) \\ (p', q') &= \sqrt{2x'}(\cos \theta', \sin \theta') \\ x + x' &= 2s_{cl} \\ \theta + \theta' &= 0 \end{aligned}$$

We therefore get $dp \wedge dq = dx \wedge d\theta = dx' \wedge d\theta' = dp' \wedge dq'$. It is interesting to note that the Weyl symbols $h_{\text{pol}}(x, \theta)$ and $h'_{\text{pol}}(x', \theta')$ are obtained from each other by the classical transformation from (x, θ) to (x', θ') . On the other hand, $h(p, q)$ and $h'(p', q')$ corresponding to the same quantum Hamiltonian in the physical subspace $0 \leq x = 2s_{cl} - x' \leq 2s_{cl}$ do not coincide, because shifting x into $x + \hbar/2$ amounts to shifting x' into $x' - \hbar/2$ instead of $x' + \hbar/2$. This implies that it is impossible to construct a quantum operator in the $2s + 1$ dimensional Hilbert space of a spin s for which both subprincipal parts of $h(p, q)$ and $h'(p', q')$ would vanish.

To formulate the Bohr-Sommerfeld rule, it is convenient to use the (p, q) coordinates when we consider a set of classical orbits which remain at a finite distance from the south pole. In these coordinates, the subleading term $\int_{C(E)} \gamma$ and the Maslov index are both continuous when $C(E)$ crosses the north pole. Going back to (x, θ) coordinates, we see that the jump in $\int_{C(E)} \gamma$ has to be compensated by a jump in the Maslov index. So the Bohr-Sommerfeld formula (54) can be expressed in (x, θ) coordinates, provided these jumps in the Maslov index are taken into account.

To check Eq.(54) we evaluate $\Phi_{Reg}(\epsilon_n)$ for the *exact* values ϵ_n and we define the defect δ_n by:

$$\Phi_{Reg}(\epsilon_n) = n + \delta_n$$

Denoting

$$\begin{aligned} I_{-1} &= \frac{1}{2\pi\hbar} \int_{C(E)} \alpha, & I_0 &= \frac{1}{2\pi} \int_{C(E)} \gamma \\ \delta_n &= I_{-1} + I_0 - (n + \frac{1}{2}), & \text{if } \epsilon_n &\leq 2\hbar\kappa s \\ \delta_n &= I_{-1} + I_0 + \frac{1}{2} - (n + \frac{1}{2}), & \text{if } 2\hbar\kappa s &\leq \epsilon_n \leq -2\hbar\kappa s \\ \delta_n &= I_{-1} + I_0 + 1 - (n + \frac{1}{2}), & \text{if } \epsilon_n &\geq -2\hbar\kappa s \end{aligned}$$

The excellent accuracy of this Bohr-Sommerfeld rule is clearly visible on Fig. 9, which shows the defect δ_n as a function of n . We see that it remains small everywhere, and we emphasize that it does not exhibit any accident when ϵ_n crosses the value $-2\kappa s_{cl}$, corresponding to the south pole. On the other hand, something special happens around $\epsilon_n = 2\kappa s_{cl}$ (the energy of the north pole), which cannot be attributed to the use of polar coordinates, but which reflects the crossing through the singular orbit associated to the pinched torus. A detailed description of the energy spectrum in the vicinity of the classical unstable point is the goal of next section.

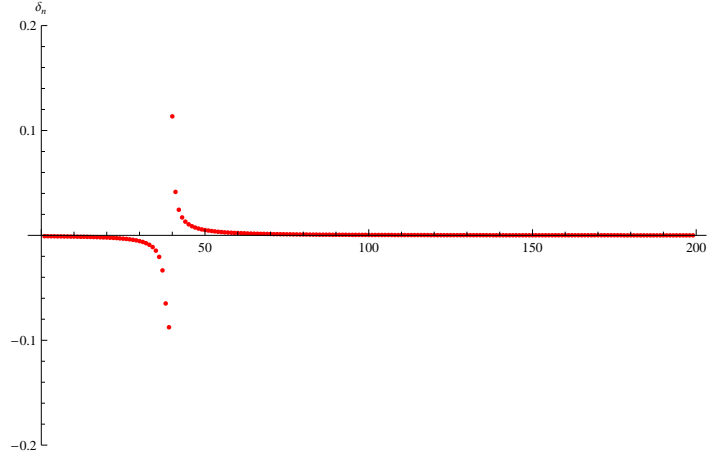


Figure 9: To test the quality of the Bohr-Sommerfeld quantization, we plot the default δ_n as a function of n which labels the energy eigenstates. We see that the accuracy of the usual Bohr-Sommerfeld rule is very good away from the critical energy. In particular there is nothing special at the south pole.

5 Generalized Bohr-Sommerfeld rule

This region of the spectrum requires a different quantization rule [16, 17, 18, 19, 20, 28, 34] because the classical motion near the turning point at x_{min} is strongly affected by the presence of the unstable point at $x = 0$. Therefore, we first need to analyze the small x behavior of the energy eigenstates, when E is close to $2\kappa s_{cl}$. In the intermediate regime, between $x_{min}(E)$ and $x_{max}(E)$, a standard WKB analysis is quite accurate. Near $x_{max}(E)$, we have a regular turning point, which can be described, as usual, by an Airy function. Gluing the wave function of the eigenstates between these three different regimes will give us the generalized Bohr Sommerfeld quantization rules.

5.1 Small x analysis

Here, we shall recast the normal form around the singular point, studied in section 2.2 within the framework of the reduced system. For this, we assume $n \ll 2s$ or $x = \hbar n \ll 2s_{cl}$. In that approximation the Schrödinger equation Eq.(50) becomes:

$$E p_n = \hbar \sqrt{2s\hbar} (n+1) p_{n+1} + \hbar \sqrt{2s\hbar} n p_{n-1} + 2\hbar \kappa (s-n) p_n \quad (56)$$

This equation is linear in n and can be solved by Laplace-Fourier transform. Letting:

$$\Psi^{\text{Small}}(\theta) = \sum_{n=0}^{\infty} p_n e^{in\theta} \quad (57)$$

the equation reads:

$$H_0 \Psi^{\text{Small}} = E \Psi^{\text{Small}}, \quad E = E_c + \hbar \epsilon$$

with:

$$H_0 = -i\hbar(\sqrt{2s_{cl}}(e^{i\theta} + e^{-i\theta}) - 2\kappa)\partial_\theta + \hbar(2\kappa s + \sqrt{2s_{cl}}e^{i\theta}) \quad (58)$$

Let us set:

$$z = e^{i\theta}, \quad \frac{d}{d\theta} = iz \frac{d}{dz}$$

the equation becomes:

$$\left[(\sqrt{2s_{cl}}(z + z^{-1}) - 2\kappa)z \frac{d}{dz} + \sqrt{2s_{cl}}z \right] \Psi^{\text{Small}} = \epsilon \Psi^{\text{Small}}$$

We are looking for a solution which is analytic in a neighborhood of the origin in the z -plane. This can be written as:

$$\Psi^{\text{Small}}(z, \epsilon) = \left(1 - \frac{z}{z_+}\right)^{\Delta_+} \left(1 - \frac{z}{z_-}\right)^{\Delta_-}$$

where z_\pm are the solutions of the second order equation already introduced before:

$$z^2 - 2\frac{\kappa}{\sqrt{2s_{cl}}}z + 1 = 0, \quad z_\pm = \frac{\kappa \pm i\Omega}{\sqrt{2s_{cl}}} = -e^{\mp i\nu}$$

and

$$\Delta_\pm = -\frac{1}{2} \mp i \frac{\epsilon - \kappa}{2\Omega} \equiv -\frac{1}{2} \mp i f(E)$$

Note that, when \hbar is small, the leading term in $f(E)$ is $(E - E_c)/2\hbar\Omega$. It is quite instructive to express directly this wave-function in the θ variable. Denoting

$$\chi(\theta) = (\cos \theta + \cos \nu)^{-1/2} \exp i \left[f(E) \log \left(\frac{|\cos \frac{\theta - \nu}{2}|}{|\cos \frac{\theta + \nu}{2}|} \right) - \frac{\theta}{2} \right]$$

we have

$$\begin{aligned} \Psi^{\text{Small}}(\theta) &= \chi(\theta), & -\pi + \nu \leq \theta \leq \pi - \nu \\ \Psi^{\text{Small}}(\theta) &= i \exp(-\pi f(E)) \chi(\theta), & \pi - \nu \leq \theta \leq \pi \\ \Psi^{\text{Small}}(\theta) &= -i \exp(-\pi f(E)) \chi(\theta), & -\pi \leq \theta \leq -\pi + \nu \end{aligned}$$

Notice that this has precisely the expected form in the semi-classical limit $\hbar \rightarrow 0$. Indeed, when $E > E_c$, the wave function is mostly confined to the interval $-\pi + \nu \leq \theta \leq \pi - \nu$, and it is exponentially small in the classically forbidden regions $\pi - \nu \leq \theta \leq \pi$ and $-\pi \leq \theta \leq -\pi + \nu$. Such exponentially small prefactor is reminiscent of the behavior of a tunneling amplitude. This is consistent with our treatment of θ as an unbounded variable, subjected to a 2π -periodic Hamiltonian. Enforcing

integer values of n requires the wave-function $\Psi^{\text{Small}}(\theta)$ to be 2π -periodic in θ . If $\Psi^{\text{Small}}(\theta)$ were identically zero in the classically forbidden intervals, its Fourier transform would develop a tail for negative values of n . So these evanescent parts of the wave-function are required in order to ensure that the wave function belongs to the physical Hilbert space $n \geq 0$. Note that when $E < E_c$, the classically forbidden region becomes the intervals $-\pi \leq \theta \leq -\pi + \nu$ and $\pi - \nu \leq \theta \leq \pi$.

In the classically allowed regions, the semi-classical wave function is expected to take the textbook form:

$$\Psi^{\text{Small}}(\theta) = a(\theta) \exp i \left(\frac{S_0(\theta)}{\hbar} + S_1(\theta) \right) \quad (59)$$

where the three functions a , S_0 and S_1 take real values. These functions satisfy the standard equations [33], involving the principal and subprincipal symbols $h^0(x, \theta) = E_c + 2\sqrt{2s_{cl}}x(\cos \theta + \cos \nu)$ and $h^1(x, \theta) = \sqrt{2s_{cl}} \cos \theta$:

$$h^0(S'_0(\theta), \theta) = E \quad (60)$$

$$\frac{d}{d\theta} (a^2(\theta) \partial_x h^0(S'_0(\theta), \theta)) = 0 \quad (61)$$

$$\partial_x h^0(S'_0(\theta), \theta) S'_1(\theta) = -h^1(S'_0(\theta), \theta) \quad (62)$$

From the above expressions for $\Psi^{\text{Small}}(\theta)$, we can check that it has *exactly* this semi-classical form. Most likely, this occurs because $\Psi^{\text{Small}}(\theta)$ is an eigenstate of a quantum Hamiltonian which is derived by symplectic reduction from the quadratic Hamiltonian of the normal form discussed in section 2.2. Quadratic Hamiltonians are particularly well-behaved with respect to the $\hbar \rightarrow 0$ limit in the sense that the Bohr-Sommerfeld formula gives the exact energy spectrum, and also that the full quantum propagator obeys similar equations as (60) and (61).

Let us now discuss the $x = n\hbar$ representation which is quite useful from the physical standpoint.

$$p^{\text{Small}}(x, \epsilon) = \oint_{C_0} \frac{dz}{2i\pi} z^{-\frac{x}{\hbar}-1} \Psi(z) = \oint_{C_0} \frac{dz}{2i\pi} z^{-\frac{x}{\hbar}-1} \left(1 - \frac{z}{z_+}\right)^{\Delta_+} \left(1 - \frac{z}{z_-}\right)^{\Delta_-}$$

where C_0 is a small contour around the origin. When E is sufficiently far (in a sense to be precised below) from its critical value E_c , we may use the saddle point approximation to evaluate $\Psi^{\text{Small}}(x, \epsilon)$. This yields again the expected semi-classical form, namely:

$$p^{\text{Small}}(x) = b(x) e^{\pm i\pi/4} \exp -i \left(\frac{W_0(x)}{\hbar} + W_1(x) \right) \quad (63)$$

where $b(x)$, $W_0(x)$ and $S_1(x)$ satisfy:

$$h^0(x, W'_0(x)) = E \quad (64)$$

$$\frac{d}{dx} (b^2(x) \partial_\theta h^0(x, W'_0(x))) = 0 \quad (65)$$

$$\partial_\theta h^0(x, W'_0(x)) W'_1(x) = -h^1(x, W'_0(x)) \quad (66)$$

Note that $W_0(x)$ is the Legendre transform of $S_0(\theta)$, that is $S'_0(\theta) = x$, $W'_0(x) = \theta$ and $S_0(\theta) + W_0(x) = x\theta$. It is interesting to write down explicitly this semi classical wave-function when $x \gg 1$. It reads:

$$p_{\text{sc}}^{\text{Small}}(x) = B_+(E) \frac{e^{-i(\pi-\nu)x/\hbar}}{(x/\hbar)^{\frac{1}{2}-if(E)}} + B_-(E) \frac{e^{i(\pi-\nu)x/\hbar}}{(x/\hbar)^{\frac{1}{2}+if(E)}}$$

where $B_-(E) = \bar{B}_+(E)$ and:

$$\frac{B_+(E)}{B_-(E)} = e^{i(\nu-\pi/2)} \exp i \left(2f(E) \log \frac{4\hbar\Omega}{|E - E_c|} + \frac{E - E_c}{\hbar\Omega} \right) \quad (67)$$

We note that the phase factor diverges when E reaches E_c . This behavior is induced by the contribution of the subprincipal symbol to the phase of the wave-function. The prefactor $\exp(i(\nu - \pi/2))$ in the above expression does not jump when E crosses the critical value E_c . This is consistent with the analysis of the previous section, because we do find a π jump in the Maslov index that is compensated by a π jump in the contribution of the subprincipal symbol.

Let us now precise the validity domain of the stationary phase approximation. When we integrate over θ to compute the Fourier transform $p^{\text{Small}}(x)$, we get an oscillating integral whose phase factor can be approximated by $\exp(iS''_0(\theta(x))(\theta - \theta(x))^2/(2\hbar))$ where $\theta(x)$ is one of the two saddle points defined implicitly by $S'_0(\theta(x)) = x$. This oscillating gaussian has a typical width $\langle \Delta\theta^2 \rangle = \hbar/|S''_0(\theta(x))|$. We find that:

$$S''_0(\theta(x)) = \frac{E - E_c}{2\sqrt{2s_{cl}}} \frac{\sin \theta}{(\cos \theta + \cos \nu)^2}$$

When E goes to E_c at fixed x , $\theta(x)$ goes to $\pm(\pi - \nu)$, because $\cos \theta + \cos \nu = E/(2\sqrt{2s_{cl}x})$. So $|S''_0(\theta(x))| \simeq 2\Omega x^2/|E - E_c|$. On the other hand, we have seen that the amplitude of $\Psi^{\text{Small}}(\theta)$ diverges when $\theta = \pm(\pi - \nu)$. The distance $\delta\theta$ between $\theta(x)$ and the closest singularity goes like $|E - E_c|/2\Omega x$. The stationary phase approximation holds as long as $\theta(x)$ is far enough from the singularities, that is if $\langle \Delta\theta^2 \rangle \ll (\delta\theta)^2$, or equivalently,

$$|E - E_c| \gg 2\hbar\Omega \quad (68)$$

When this condition is not fulfilled, the stationary phase approximation breaks down. The dominant contribution to $p^{\text{Small}}(x)$ comes from the vicinity of $\theta = \pm(\pi - \nu)$. We have therefore to consider a different asymptotic regime, where \hbar goes to 0 while $\epsilon = (E - E_c)/\hbar$ remains fixed. In this case, the two exponents Δ_+ , Δ_- are fixed, and the only large parameter in the Fourier integral giving $p^{\text{Small}}(x)$ is x/\hbar . One then obtains:

$$p^{\text{Small}}(x) = A_+(E) \frac{e^{-i(\pi-\nu)x/\hbar}}{(x/\hbar)^{\frac{1}{2}-if(E)}} + A_-(E) \frac{e^{i(\pi-\nu)x/\hbar}}{(x/\hbar)^{\frac{1}{2}+if(E)}} \equiv p_+^{\text{Small}}(x) + p_-^{\text{Small}}(x) \quad (69)$$

with $A_-(E) = \bar{A}_+(E)$ and:

$$\frac{A_+(E)}{A_-(E)} = e^{i(\nu-\pi/2)} \frac{\Gamma(\frac{1}{2} - if(E))}{\Gamma(\frac{1}{2} + if(E))} \exp i(2f(E) \log(2 \sin \nu)) \quad (70)$$

This analysis first shows that, in spite of the breakdown of the stationary phase approximation, $p^{\text{Small}}(x)$ is still given at large x by a sum of two semi-classical wave-functions associated to the same principal and subprincipal symbols h^0 and h^1 . This implies that there will be a perfect matching between $p^{\text{Small}}(x)$ and the WKB wave functions built at finite x from the full classical Hamiltonian. This will be discussed in more detail below. The only modification to the conventional WKB analysis lies in the phase factor A_+/A_- between the ongoing and outgoing amplitudes, which differs markedly from the semi-classical B_+/B_- . In particular, we see that the full quantum treatment at fixed ϵ provides a regularization of the divergence coming from the subprincipal symbol. Indeed, the singular factor $\log(4\hbar\Omega/|E - E_c|)$ is replaced by the constant $\log(2 \sin \nu)$. Such a phenomenon has been demonstrated before for various models [20, 28].

5.2 WKB analysis

We return to the Schrödinger equation:

$$(x + \hbar)\sqrt{2s_{cl} - x} p(x + \hbar) + x\sqrt{2s_{cl} + \hbar - x} p(x - \hbar) - 2\kappa x p(x) = \hbar\epsilon p(x) \quad (71)$$

where:

$$\hbar\epsilon = E - E_c$$

We try to solve this equation by making the WKB Ansatz:

$$p^{\text{WKB}}(x) = e^{\frac{i}{\hbar}(W_0(x) + \hbar W_1(x))} b(x)$$

Expanding in \hbar , to order \hbar^0 we find

$$x\sqrt{2s_{cl} - x} \cos W'_0 - \kappa x = 0 \quad (72)$$

which is nothing but the Hamilton-Jacobi equation on the critical variety. It is identical to Eq. (64) where $h^0(x, \theta)$ is the complete principal symbol, and the energy is taken to be E_c . In this procedure, the energy difference $\hbar\epsilon$ is viewed as a perturbation, which can be treated by adding the constant term $-\epsilon$ to the complete subprincipal symbol $h^1(x, \theta)$. Alternatively, we may write the Hamilton-Jacobi equation as:

$$e^{iW'_0} = z(x), \quad z^2(x) - \frac{2\kappa}{\sqrt{2s_{cl} - x}} z(x) + 1 = 0$$

The solution of the quadratic equation is:

$$z_{\pm}(x) = \frac{1}{\sqrt{2s_{cl} - x}} (\kappa \pm i\sqrt{\Omega^2 - x}) = \left(\frac{\kappa \pm i\sqrt{\Omega^2 - x}}{\kappa \mp i\sqrt{\Omega^2 - x}} \right)^{1/2} \quad (73)$$

so that $z_{\pm}(x)|_{x=0} = e^{\pm i(\pi-\nu)}$. Hence:

$$e^{-\frac{i}{\hbar}W_0(x)} = e^{\mp \frac{i}{\hbar} \left(\pi x + \kappa \sqrt{\Omega^2 - x} + \frac{i}{2}(2s_{cl} - x) \log \frac{\kappa + i\sqrt{\Omega^2 - x}}{\kappa - i\sqrt{\Omega^2 - x}} \right)} \quad (74)$$

where the two signs refer to the two branches of the classical trajectory. Notice that they also correspond to the two determinations of the square root $\sqrt{\Omega^2 - x}$.

At the next order in \hbar the equation for $b(x)$ is:

$$\frac{d}{dx} \left(b^2(x) x \sqrt{\Omega^2 - x} \right) = 0 \quad (75)$$

Therefore, we may choose $b(x) = (x\sqrt{\Omega^2 - x})^{-1/2}$.

The correction $W_1(x)$ to the phase function satisfies Eq. (66) with $h^1(x, \theta)$ replaced by $h^1(x, \theta) - \epsilon$, that is:

$$\partial_{\theta} h^0(x, W_0'(x)) W_1'(x) = -h^1(x, W_0'(x)) + \epsilon$$

$W_1'(x)$ is the sum of two terms, $W_1'(x) = -\gamma(x) + \epsilon \delta\beta(x)$, where $\gamma(x)dx$ is simply the one-form γ defined by Eq. (53), evaluated on the critical trajectory, and $\delta\beta(x) = (\partial_{\theta} h^0(x, W_0'(x)))^{-1}$. To understand better the meaning of $\delta\beta(x)$, we start with the action integral $\int_{C(E)} \beta$, where $\beta = \theta dx$ is closely related to the canonical 1-form $\alpha = x d\theta$, because $\alpha + \beta = d(x\theta)$. Note that, by contrast to α , β is defined on the sphere only after choosing a determination of the longitude θ . Let us now study the variation of this action integral when E moves away from E_c and is changed into $E_c + \hbar\epsilon$. We have:

$$\int_{C(E_c + \hbar\epsilon)} \beta - \int_{C(E_c)} \beta = \hbar\epsilon \int_{C(E_c)} \frac{\partial \theta}{\partial E} dx$$

But $\theta(x, E)$ satisfies $h^0(x, \theta(x, E)) = E$, so:

$$\partial_{\theta} h^0(x, \theta(x, E)) \frac{\partial \theta}{\partial E}(x, E) = 1$$

and finally:

$$\int_{C(E_c + \hbar\epsilon)} \beta - \int_{C(E_c)} \beta = \hbar\epsilon \int_{C(E_c)} \delta\beta(x) dx$$

Explicitely, the equation for $W_1(x)$ reads:

$$W_1'(x) = \frac{\pm 1}{2\sqrt{\Omega^2 - x}} \left(\frac{\kappa}{2(2s_{cl} - x)} + \frac{\kappa - \epsilon}{x} \right) \quad (76)$$

So we have:

$$e^{-iW_1(x)} = \exp \left(\pm \frac{1}{4} \log \frac{\kappa + i\sqrt{\Omega^2 - x}}{\kappa - i\sqrt{\Omega^2 - x}} \mp i \frac{\epsilon - \kappa}{2\Omega} \log \frac{\Omega + \sqrt{\Omega^2 - x}}{\Omega - \sqrt{\Omega^2 - x}} \right) \quad (77)$$

We can now expand $p^{\text{WKB}}(x)$ when x is small. We find:

$$p_{\pm}^{\text{WKB}}(x) \simeq A_{\pm}^{\text{WKB}}(\epsilon) \frac{e^{\mp i(\pi-\nu)\frac{x}{\hbar}}}{(x/\hbar)^{\frac{1}{2}\mp if(E)}} \quad (78)$$

where:

$$A_{\pm}^{\text{WKB}}(\epsilon) = \frac{1}{\sqrt{\Omega}} e^{\mp i \left[\frac{\kappa\Omega}{\hbar} + (2s+\frac{1}{2})\nu + \frac{\epsilon-\kappa}{2\Omega} \log\left(\frac{4\Omega^2}{\hbar}\right) \right]}$$

Notice that the phase factor is the sum of two terms which have simple geometrical interpretations:

$$S_{cl}^+ = \kappa\Omega + 2s_{cl}\nu = \pi\Omega^2 - \int_0^{\Omega^2} \theta(x)dx = \int_{C_+} \alpha$$

is the classical action computed on the upper half of the classical trajectory, and

$$\frac{\nu}{2} + \frac{\epsilon-\kappa}{2\Omega} \log\left(\frac{4\Omega^2}{\hbar}\right) = \int_0^{\Omega^2} \tilde{\gamma}(x)dx$$

is the regularized integral of the subprincipal symbol $\tilde{\gamma}(x) = \gamma(x) - \epsilon\delta\beta(x)$ on the same trajectory:

$$\int_0^{\Omega^2} \tilde{\gamma}(x)dx = \lim_{x_A \rightarrow 0} \left(\int_{x_A}^{\Omega^2} \tilde{\gamma}(x)dx + f(E) \log \frac{x_A}{\hbar} \right)$$

Similarly, setting $x = \Omega - |\xi|$ and expanding in $\frac{|\xi|}{\Omega}$ and $\frac{|\xi|}{\kappa}$ we find to leading order:

$$p_{\pm}^{\text{WKB}}(x) \simeq \frac{1}{\Omega|\xi|^{1/4}} e^{\pm \frac{2i}{3\hbar\kappa} |\xi|^{3/2} \pm i \left(\frac{1}{2\kappa} - \frac{\epsilon-\kappa}{\Omega^2} \right) |\xi|^{1/2}} \quad (79)$$

The relevant wave function is of course a linear combination of $p_{\pm}^{\text{WKB}}(x)$.

5.3 Airy function analysis

Again, we start with the Schrödinger equation Eq. (71). We set:

$$p^{\text{Airy}}(x) = (-1)^n \tilde{p}^{\text{Airy}}(x), \quad x = n\hbar$$

$$(x + \hbar)\sqrt{2s_{cl} - x} \tilde{p}^{\text{Airy}}(x + \hbar) + x\sqrt{2s_{cl} + \hbar - x} \tilde{p}^{\text{Airy}}(x - \hbar) + 2\kappa x \tilde{p}^{\text{Airy}}(x) = -\hbar\epsilon \tilde{p}^{\text{Airy}}(x) \quad (80)$$

and we expand $x = \Omega^2 + \xi$, keeping the terms linear in ξ . Remembering that $\sqrt{\kappa^2} = -\kappa$, we find:

$$\frac{d^2}{d\xi^2} \tilde{p}^{\text{Airy}} + \frac{1}{\Omega^2} \left(1 - \frac{\Omega^2}{2\kappa^2} \right) \frac{d}{d\xi} \tilde{p}^{\text{Airy}} - \frac{1}{\hbar^2 \kappa \Omega^2} \left(\hbar\epsilon - \frac{\hbar\Omega^2}{2\kappa} - \hbar\kappa - \frac{\Omega^2}{\kappa} \xi \right) \tilde{p}^{\text{Airy}} = 0$$

The unique solution which decreases exponentially in the classically forbidden region $\xi > 0$ is proportional to the Airy function:

$$\tilde{p}^{\text{Airy}}(\xi) = e^{-c\xi} \text{Airy}(a^{1/3}(\xi - b))$$

where:

$$a = \frac{1}{\hbar^2 \kappa^2}, \quad b = \hbar \left(\frac{1}{2} - \frac{\kappa(\epsilon - \kappa)}{\Omega^2} \right), \quad c = \frac{1}{2\Omega^2} \left(1 - \frac{\Omega^2}{2\kappa^2} \right)$$

When $\xi < 0$ it behaves like:

$$\frac{\sin\left(\frac{2}{3}|X|^{2/3} + \frac{\pi}{4}\right)}{|X|^{1/4}}, \quad X = a^{1/3}(\xi - b)$$

We expand in $\frac{|\xi|}{\kappa}$ and $\frac{|\xi|}{\Omega}$. One has:

$$\frac{2}{3}|X|^{3/2} = -\frac{2}{3\hbar\kappa}|\xi|^{3/2} - \left(\frac{1}{2\kappa} - \frac{(\epsilon - \kappa)}{\Omega^2} \right) |\xi|^{1/2}$$

In that approximation $e^{-c\xi} \simeq 1$, and we get:

$$\tilde{p}^{\text{Airy}}(\xi) = C \frac{\sin\left(\frac{2}{3\hbar\kappa}|\xi|^{3/2} + \left(\frac{1}{2\kappa} - \frac{(\epsilon - \kappa)}{\Omega^2}\right)|\xi|^{1/2} - \frac{\pi}{4}\right)}{\sqrt{\pi}|\xi|^{1/4}} \quad (81)$$

5.4 Gluing the parts together

The small x analysis gave:

$$p(x) = p_+^{\text{Small}}(x) + p_-^{\text{Small}}(x)$$

which is valid when $x \ll 2s_{cl}$. In an intermediate regime, both the small x and the WKB approximation are valid at the same time, as can be seen by comparing Eq. (69) and Eq. (78). So we can glue these two wave-functions as follows:

$$p(x) = \frac{A_+^{\text{Small}}(\epsilon)}{A_+^{\text{WKB}}(\epsilon)} p_+^{\text{WKB}}(x) + \frac{A_-^{\text{Small}}(\epsilon)}{A_-^{\text{WKB}}(\epsilon)} p_-^{\text{WKB}}(x)$$

We can now prolongate the $p_{\pm}^{\text{WKB}}(x)$ functions up to the region $x \simeq \Omega^2 - |\xi|$. Recalling the asymptotic form of the WKB wave function in that region Eq. (79), we find

$$\begin{aligned} p(x) &\simeq \frac{A_+^{\text{Small}}(\epsilon)}{A_+^{\text{WKB}}(\epsilon)} \frac{1}{\Omega|\xi|^{1/4}} e^{\frac{2i}{3\hbar\kappa}|\xi|^{3/2} + i\left(\frac{1}{2\kappa} - \frac{\epsilon - \kappa}{\Omega^2}\right)|\xi|^{1/2}} \\ &\quad + \frac{A_-^{\text{Small}}(\epsilon)}{A_-^{\text{WKB}}(\epsilon)} \frac{1}{\Omega|\xi|^{1/4}} e^{-\frac{2i}{3\hbar\kappa}|\xi|^{3/2} - i\left(\frac{1}{2\kappa} - \frac{\epsilon - \kappa}{\Omega^2}\right)|\xi|^{1/2}} \end{aligned}$$

This has to be compatible with the Airy asymptotic formula which embodies the boundary conditions Eq. (81). Hence we find the condition:

$$\frac{A_+^{\text{Small}}(\epsilon)}{A_-^{\text{Small}}(\epsilon)} \frac{A_-^{\text{WKB}}(\epsilon)}{A_+^{\text{WKB}}(\epsilon)} \frac{e^{i\frac{\pi}{4}}}{e^{-i\frac{\pi}{4}}} = -1 \quad (82)$$

This equation determines the energy parameter ϵ and is the generalized Bohr-Sommerfeld condition. Given the fact that:

$$\begin{aligned} \frac{A_+^{\text{Small}}(\epsilon)}{A_-^{\text{Small}}(\epsilon)} &= e^{i(\nu - \frac{\pi}{2})} \frac{\Gamma\left(\frac{1}{2} - i\frac{\epsilon - \kappa}{2\Omega}\right)}{\Gamma\left(\frac{1}{2} + i\frac{\epsilon - \kappa}{2\Omega}\right)} e^{i\frac{\epsilon - \kappa}{\Omega} \log\left(\frac{2\Omega}{\sqrt{2s_{cl}}}\right)} \\ \frac{A_+^{\text{WKB}}(\epsilon)}{A_-^{\text{WKB}}(\epsilon)} &= e^{-2i\left[\frac{2\kappa\Omega}{\hbar} + (4s+1)\nu + \frac{\epsilon - \kappa}{\Omega} \log\left(\frac{4\Omega^2}{\hbar}\right)\right]} \end{aligned}$$

Eq.(82) becomes:

$$\frac{\Gamma\left(\frac{1}{2} - i\frac{\epsilon - \kappa}{2\Omega}\right)}{\Gamma\left(\frac{1}{2} + i\frac{\epsilon - \kappa}{2\Omega}\right)} e^{i\left[\frac{2\kappa\Omega}{\hbar} + 2(2s+1)\nu + \frac{\epsilon - \kappa}{\Omega} \log\left(\frac{8\Omega^3}{\hbar\sqrt{2s_{cl}}}\right)\right]} = -1 \quad (83)$$

Taking the logarithm, we find the quantization condition:

$$\Phi_{\text{Sing}}(\epsilon_n) = 2\pi \left(n + \frac{1}{2} \right), \quad n \in Z, \quad E_n = 2\kappa s_{cl} + \hbar\epsilon_n \quad (84)$$

where:

$$\Phi_{\text{Sing}}(\epsilon) = -i \log \frac{\Gamma\left(\frac{1}{2} - i\frac{\epsilon - \kappa}{2\Omega}\right)}{\Gamma\left(\frac{1}{2} + i\frac{\epsilon - \kappa}{2\Omega}\right)} + \frac{2\kappa\Omega}{\hbar} + 2(2s+1)\nu + \frac{\epsilon - \kappa}{\Omega} \log\left(\frac{8\Omega^3}{\hbar\sqrt{2s_{cl}}}\right)$$

To test this condition, we can compute $\delta_n = \Phi(\epsilon_n^{\text{exact}}) - 2\pi\left(n + \frac{1}{2}\right)$ for the exact values of the energies. In Figure 10, we plot δ_n as a function of n , using for $\Phi(\epsilon)$ both the usual Bohr-Sommerfeld function:

$$\Phi_{\text{Reg}}(\epsilon) = \frac{1}{\hbar} \int_{C(E)} \alpha + \int_{C(E)} \gamma$$

and the function $\Phi_{\text{Sing}}(\epsilon)$. Near the singularity, the singular Bohr-Sommerfeld condition is much more accurate.

In Figure 11 a typical example of the components of the eigenvectors is shown, comparing with the exact result obtained by direct diagonalization of the Jacobi matrix Eq. (50) and the various results corresponding to the different approximations: small x , WKB, and Airy. The agreement is very good.

From Eq. (84) we can compute the level spacing between two successive energy levels. It is given by:

$$\epsilon_{n+1} - \epsilon_n = \frac{2\pi}{\Phi'_{\text{Sing}}(\epsilon_n)} = \frac{2\pi\Omega}{\log\left(\frac{8\Omega^3}{\hbar\sqrt{2s_{cl}}}\right) - \Psi'\left(\frac{\epsilon - \kappa}{2\Omega}\right)} \quad (85)$$

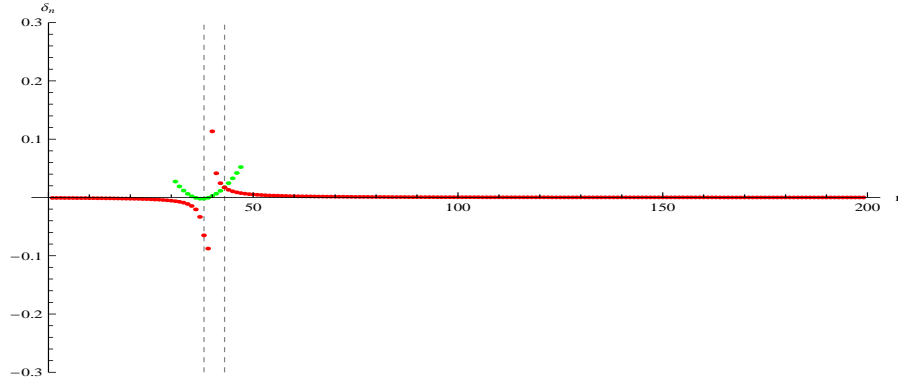


Figure 10: To compare the usual and the singular Bohr-Sommerfeld rules, the default δ_n is plotted as a function of n . The red dots are obtained by using the usual Bohr Sommerfeld rule, while the green dots are obtained by using $\Phi_{Sing}(\epsilon)$. The dashed vertical lines represent the interval $|E - E_c| < 2\hbar\Omega$ of validity of the singular Bohr-Sommerfeld rule.

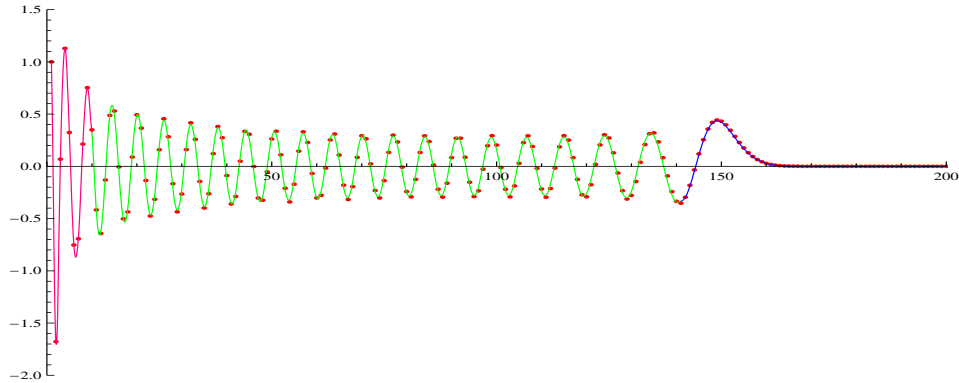


Figure 11: The components of an eigenvector close to the critical level. The dots are the exact result. The red curve is the result of the small x analysis. The green curve is the WKB result and the blue curve is the Airy result.

where we defined

$$\Psi'(x) = \frac{i}{2} \frac{d}{dx} \log \frac{\Gamma(\frac{1}{2} - ix)}{\Gamma(\frac{1}{2} + ix)}$$

This function has a sharp minimum located at $x = 0$ where it takes the value $-(\gamma + 2 \log 2)$ where γ is Euler's constant, see Fig. 12. Hence to leading order, the smallest energy spacing is:

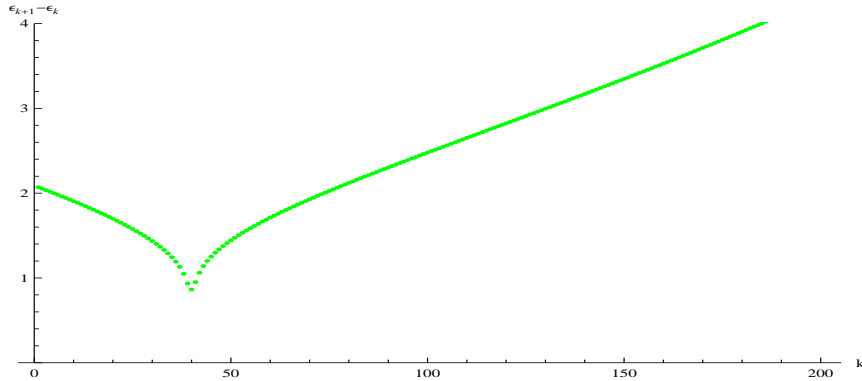


Figure 12: The energy level spacing $\epsilon_{k+1} - \epsilon_k$ as a function of the state label k . This plot shows clearly the accumulation of energy levels in the vicinity of the critical point.

$$\Delta\epsilon \simeq \frac{2\pi\Omega}{|\log \hbar|}$$

A detailed analysis of the level spacing in the vicinity of the critical level has been given recently [34], where it has been applied to the description of the long time dynamics of the system.

6 Evolution of the oscillator energy

Once the eigenvectors and eigenvalues are known, we can compute the time evolution of the oscillator energy:

$$\bar{x}(t) = \langle s | e^{i\frac{tH}{\hbar}} b^\dagger b e^{-i\frac{tH}{\hbar}} | s \rangle$$

Since the observable $b^\dagger b$ commutes with H_1 , its matrix elements between eigenstates of H_1 with different eigenvalues vanish. Because $|s\rangle$ is an eigenvector of H_1 with eigenvalue $\hbar s$, we can therefore restrict ourselves to this eigenspace of H_1 . The time evolution can be computed numerically by first decomposing the initial state on the eigenvector basis:

$$|s\rangle = \sum_n c_n |\Psi(E_n)\rangle \tag{86}$$

so that the wave-function at time t is:

$$|\Psi(t)\rangle = \sum_n c_n e^{-iE_n t/\hbar} |\Psi(E_n)\rangle$$

In the stable regime $\kappa^2 > 2s_{cl}$, we get quite regular oscillations with a rather small amplitude as shown in Figure 13.

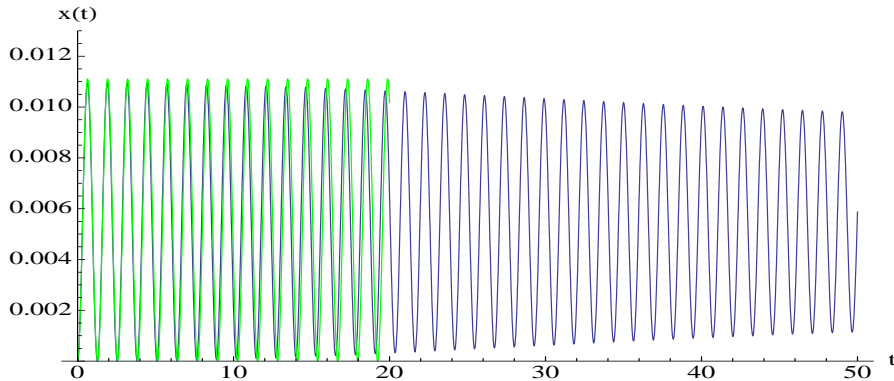


Figure 13: The excitation number of the oscillator as function of time in the stable case. The green curve is the small time result Eq. (98). ($\hbar^{-1} = s = 30$, $\kappa = -2\sqrt{2s_{cl}}$, $s_{cl} = 1$). Notice that the vertical amplitude is about one hundred times smaller than in the unstable case (compare with Fig. 14).

By contrast, in the unstable regime $\kappa^2 < 2s_{cl}$, it is energetically favorable to excite the oscillator, and we get a succession of well separated pulses shown in Figure 14. Note that the temporal succession of these pulses displays a rather well defined periodicity, but the fluctuations from one pulse to another are relatively large. The remaining part of this paper is an attempt to understand the main features of this evolution.

On Figure 15 we show the coefficients $|c_n|$. Only those eigenstates whose energy is close to the critical classical energy E_c contribute significantly. A good estimate of the energy width of the initial state $|s\rangle$ is given by $\Delta E = (\langle s|H^2|s\rangle - \langle s|H|s\rangle^2)^{1/2}$. From Eq. (50), we find:

$$\Delta E = \hbar\sqrt{2s_{cl}} = \hbar\Omega/\sin\nu \quad (87)$$

Comparing with the criterion $|\Delta E| \gg 2\hbar\Omega$ for the validity of the stationary phase approximation, we see that most of the eigenstates which have a significant weight in the spectral decomposition of the initial state actually belong to the singular Bohr-Sommerfeld regime.

An important consequence of this observation is that we can compute $\bar{x}(t)$ by considering only the few relevant states. The result is shown in Figure 16 for a spin $s = 30$. We retained only six

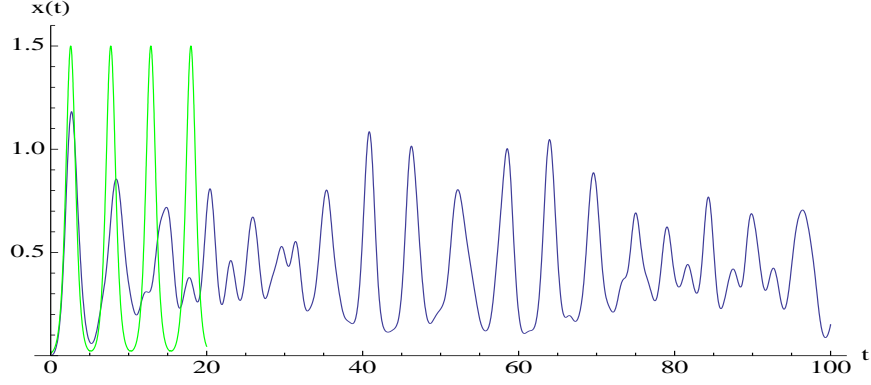


Figure 14: The excitation number of the oscillator as function of time in the unstable case. ($\hbar^{-1} = s = 30$, $\kappa = -0.5\sqrt{2s_{cl}}$, $s_{cl} = 1$). It clearly shows an aperiodic succession of pulses. The green curve is the semiclassical result Eq. (102).

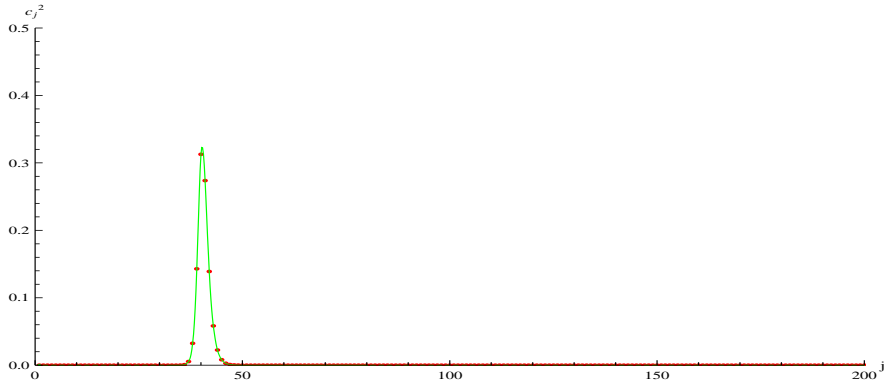


Figure 15: The coefficients of the expansion of the initial state $|s\rangle$ on the eigenvectors $|\Psi(E_n)\rangle$. The red dots are the exact values. We see that only eigenvectors close to the critical level contribute significantly. The curve is given by Eq. (89), which is deduced from the knowledge of the short time evolution. The agreement between this approximate result and the exact one is remarkable, even in the immediate vicinity of the critical level.

states and superposed the result to the exact curve obtained by keeping the 61 states. We can hardly see any difference between the two curves.

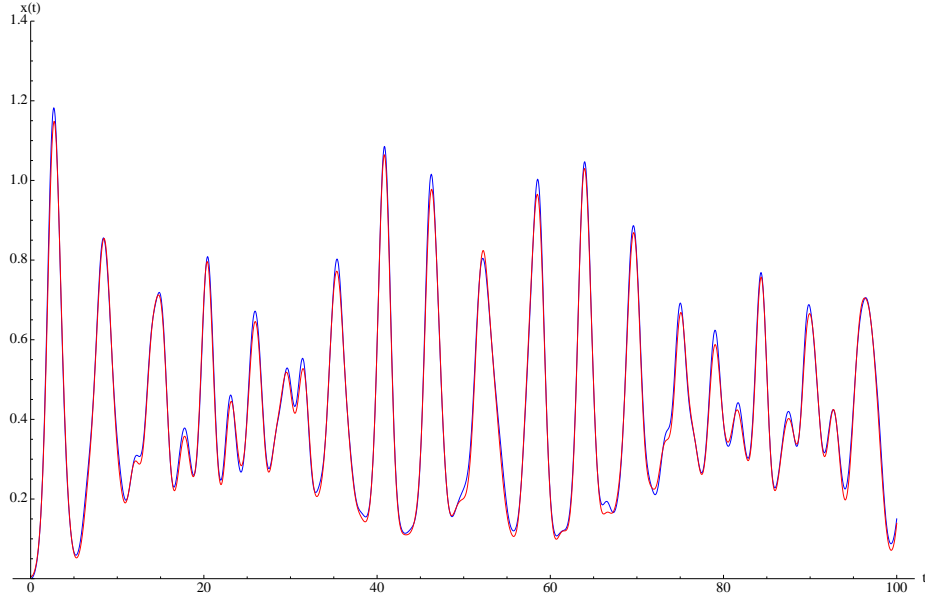


Figure 16: The excitation number of the oscillator as function of time for $s = 30$. The blue curve is the exact result, and the red curve is obtained by keeping only 6 energy eigenstates.

We can compute the coefficients $|c_n|$ of the decomposition of the initial state $|s\rangle$. From Eq. (86), we have:

$$\langle s|e^{-i\frac{Ht}{\hbar}}|s\rangle = \sum_n e^{-i\frac{E_n t}{\hbar}} |c_n|^2 \simeq \int_{-\infty}^{\infty} e^{-i\frac{Et}{\hbar}} |c(E)|^2 \rho(E) dE \quad (88)$$

where we have approximated the sum over discrete energy levels by an integral. Since we already know that the integral is concentrated around the critical energy E_c , the density $\rho(E)$ can be computed from the singular Bohr-Sommerfeld phase eq.(84):

$$\rho(E) = \frac{dn}{dE} = \frac{1}{2\pi} \frac{d}{dE} \Phi_{Sing}(E) = \frac{1}{2\pi\hbar} \frac{d}{d\epsilon} \Phi_{Sing}(\epsilon)$$

On the other hand, since

$$|s\rangle = \frac{e_0}{\|e_0\|}$$

where e_0 is the state Eq. (42) with the oscillator in its ground state, we get:

$$\langle s|e^{-i\frac{Ht}{\hbar}}|s\rangle = \frac{1}{2\pi} \int_0^{2\pi} \Psi(\theta, t) d\theta = p_0(t)$$

where $\Psi(\theta, t)$ is the solution of the Schrödinger equation with initial condition $\Psi(\theta, t)|_{t=0} = 1$. Inverting the Fourier transform in Eq. (88), we arrive at:

$$|c(E)|^2 \rho(E) = \frac{1}{2\pi\hbar} \int_{-\infty}^{\infty} e^{i\frac{Et}{\hbar}} p_0(t) dt$$

Taking for $p_0(t)$ the small time expression Eq. (96), which is valid for times $t < t_0 \simeq \frac{|\log \hbar|}{2\Omega}$, we expect to find an expression valid in the energy interval $|E - E_c| > 2\Omega \frac{\hbar}{|\log \hbar|}$ i.e. for energies far enough from the critical energy. However because of the factor $1/|\log \hbar|$ this interval covers most of the range Eq. (87) where we expect $c(E)$ to be substantially non zero. Notice also that $\frac{\hbar}{|\log \hbar|}$ is the order of magnitude of level spacing in the critical region, so that the interval where the use of the small time wave function is not legitimate contains at most a few levels. Explicitly, computing the Fourier transform of Eq. (96), we find:

$$|c(E)|^2 \rho(E) = \frac{1}{\hbar\sqrt{2s_{cl}}} \frac{e^{-\frac{\nu\alpha(E)}{\hbar\Omega}}}{1 + e^{-\frac{\pi\alpha(E)}{\hbar\Omega}}} \quad (89)$$

where:

$$\alpha(E) = E - E_c - \hbar\kappa$$

The coefficients $|c(E)|^2$ computed with this formula are shown in Fig. 15. The agreement with the exact coefficients is excellent.

For longer time scales, we may also infer that the quantum dynamics exhibits the Bohr frequencies that can be deduced from the singular Bohr-Sommerfeld quantization rule (84). As shown before, the typical spacing between these energy levels is given by $\Delta\epsilon \simeq \frac{2\pi\Omega}{|\log \hbar|}$. This corresponds to a fundamental period $\Delta t \simeq |\log \hbar|/\Omega$. The fact that the energy levels are not equally spaced, as shown on Figure 12 is responsible for the aperiodic behavior on time scales larger than Δt . Systematic procedures to analyze the long time behavior, starting from a nearly equidistant spectrum have been developed [35], but we have not yet attempted to apply them to the present problem. Note that the quantum dynamics in the vicinity of classically unstable equilibria has received a lot of attention in recent years [36, 37].

Instead, motivated by the analysis of the previous section, we now present a discussion of the time evolution in the semi-classical regime. As for the stationary levels, we show that we have to treat separately the initial evolution, when x is still small and the system is close to the unstable point, and the motion at later times, for which the usual WBK approach is quite reliable. As we demonstrate, this allows us to predict the appearance of pulses, together with their main period Δt . This generalizes the early study by Bonifacio and Preparata [9], who focussed on the $\kappa = 0$ case.

6.1 Small time analysis

Another expression for the mean oscillator energy is:

$$\bar{x}(t) = \hbar \sum_{n=0}^{2s} n |p_n(t)|^2$$

where $p_n(t)$ is the solution of Eq. (47) with boundary condition:

$$p_n(t)|_{t=0} = \delta_{n,0}$$

For small time, $p_n(t)$ will be significantly different from zero only for small n . So in Eq. (47) we may assume $n \ll 2s$. The equation becomes:

$$i\hbar \frac{\partial p_n}{\partial t} = \hbar\sqrt{2s\hbar}(n+1)p_{n+1} + \hbar\sqrt{2s\hbar}np_{n-1} + 2\hbar\kappa(s-n)p_n \quad (90)$$

As for the stationary case, this equation is linear in n and can be solved by Laplace-Fourier transform. We define:

$$\Psi(\theta, t) = \sum_{n=0}^{\infty} p_n(t)e^{in\theta}, \quad \Psi(\theta, t)|_{t=0} = 1 \quad (91)$$

The time evolution is given by:

$$\partial_t \Psi = -(\sqrt{2s_{cl}}(e^{i\theta} + e^{-i\theta}) - 2\kappa)\partial_\theta \Psi - i(2\kappa s + \sqrt{2s_{cl}}e^{i\theta})\Psi \quad (92)$$

This equation can be solved by the method of characteristics. We introduce the function $y(\theta)$ defined by:

$$\frac{dy}{d\theta} = \frac{1}{\sqrt{2s_{cl}}(e^{i\theta} + e^{-i\theta}) - 2\kappa}$$

Explicitly:

$$y(\theta) = \frac{1}{2\Omega} \log \frac{e^{i\theta} + e^{i\nu}}{e^{i\theta} + e^{-i\nu}}, \quad \text{or else} \quad e^{i\theta} = \frac{1}{\sqrt{2s_{cl}}} \left(\kappa + i\Omega \frac{\cosh \Omega y}{\sinh \Omega y} \right)$$

The time dependent Schrödinger equation becomes:

$$\partial_t \Psi + \partial_y \Psi = -i(2s+1)\kappa\Psi + \Omega \frac{\cosh \Omega y}{\sinh \Omega y} \Psi$$

whose solution reads:

$$\Psi(y, t) = e^{-i\kappa(2s+1)t} \frac{\sinh \Omega y}{\sinh \Omega(y-t)} \Psi(y-t, 0)$$

Imposing the initial condition Eq. (91) yields $\Psi(y-t, 0) = 1$ and then:

$$\Psi(y, t) = e^{-i\kappa(2s+1)t} \frac{\sinh \Omega y}{\sinh \Omega(y-t)}$$

Returning to the variable θ , we get:

$$\Psi(\theta, t) = e^{-i\kappa(2s+1)t} \frac{e^{i\nu} - e^{-i\nu}}{e^{i\nu-\Omega t} - e^{-i\nu+\Omega t}} \frac{1}{1 - \frac{e^{\Omega t} - e^{-\Omega t}}{e^{i\nu-\Omega t} - e^{-i\nu+\Omega t}} e^{i\theta}} \quad (93)$$

As for the stationary case, we note that this wave-function has exactly the form dictated by semi-classical analysis, where the full symbol associated to Eqs. (90),(92) is $h(x, \theta) = 2\sqrt{2s_{cl}}(x + \hbar/2)(\cos \theta + \cos \nu)$, after we have subtracted the energy E_c of the unstable point. The generalization of Eq. (60) to the time dependent case is:

$$h^0(\partial_\theta S_0(\theta, t), \theta) + \partial_t S_0(\theta, t) = 0 \quad (94)$$

But since Ψ is independent of θ at $t = 0$, $\partial_\theta S_0(\theta, t = 0) = 0$, which means classically that the trajectory begins at $x = 0$. But because of the form of h^0 , we get $h^0(\partial_\theta S_0(\theta, t = 0), \theta) = 0$ for any θ , which implies that $\partial_t S_0(\theta, t = 0) = 0$. This shows that $S_0(\theta, t) = 0$ identically, in agreement with the fact that a classical trajectory starting at $x = 0$ stays there for ever! So the time evolution manifested in Eq. (93) is of purely quantum nature, and it is encoded in the evolution of the amplitude $a(\theta, t)$ and the subleading phase $S_1(\theta, t)$. Writing $\Psi = a(\theta, t) \exp(iS_1(\theta, t))$, the next order in \hbar gives:

$$\partial_x h^0(0, \theta) \partial_\theta \Psi + \partial_t \Psi + \frac{1}{2} \frac{d}{d\theta} (\partial_x h^0(0, \theta))|_t \Psi + i h^1(0, \theta) \Psi = 0 \quad (95)$$

A simple check shows this is exactly the same equation as (92) without the term $-i2\kappa s \Psi$, due to the subtraction of the energy E_c . Expanding in $e^{i\theta}$ we find:

$$p_n(t) = e^{-i\kappa(2s+1)t} \frac{e^{i\nu} - e^{-i\nu}}{e^{i\nu-\Omega t} - e^{-i\nu+\Omega t}} \left[\frac{e^{\Omega t} - e^{-\Omega t}}{e^{i\nu-\Omega t} - e^{-i\nu+\Omega t}} \right]^n \quad (96)$$

It is instructive to consider the large n limit. Then $p_n(t)$ is proportional to $\exp[-\frac{i}{\hbar}(\kappa(2s_{cl} + \hbar)t + (\pi - \nu)x)]$. This is the dominant phase factor for a WKB state of energy $E = E_c$ which is concentrated on the outgoing branch of the critical classical trajectory. Note that there also appears a quantum correction to the energy, corresponding to a finite $\epsilon = \kappa$. On the physical side, this is quite remarkable, because we have just seen that the short time evolution is driven by purely quantum fluctuations, formally described by the subprincipal symbol. Nevertheless, the subsequent evolution is quite close to the classical critical trajectory, because the energy distribution of the initial state is quite narrow, as we have discussed.

Further information is obtained by looking at the probability distribution of the number of emitted quantas:

$$|p_n(t)|^2 = \frac{\Omega^2}{\Omega^2 + 2s_{cl} \sinh^2 \Omega t} \left[\frac{2s_{cl} \sinh^2 \Omega t}{\Omega^2 + 2s_{cl} \sinh^2 \Omega t} \right]^n$$

This is of the form:

$$|p_n(t)|^2 \simeq e^{-\beta(t)n}, \quad \beta(t) = \log \left(1 + \frac{\Omega^2}{2s_{cl} \sinh^2 \Omega t} \right)$$

Hence we have a *thermal* distribution with a time-dependent effective temperature. Such behavior is due to the strong entanglement between the spin and the oscillator. In fact we somehow expect that quantum effects, such as entanglement, are likely to be magnified in situations where there is an important qualitative difference between the classical and the quantum evolutions.

It is now simple to compute the mean number of molecules produced in this small time regime. We find:

$$\bar{x}(t) = 2\hbar s_{cl} \frac{\sinh^2 \Omega t}{\Omega^2}, \quad \Omega = \sqrt{2s_{cl} - \kappa^2} \quad (97)$$

The small time approximation is valid as long as the number of molecules is small and will break after a time t_0 such that $\bar{x}(t_0) \simeq 1$. To leading order in \hbar , this time scale is:

$$t_0 \simeq -\frac{1}{2\Omega} \log \hbar$$

Note that in the *stable* case, we change Ω into $i\Omega$ and then:

$$\bar{x}(t) = 2\hbar s_{cl} \frac{\sin^2 \Omega t}{\Omega^2}, \quad \Omega = \sqrt{\kappa^2 - 2s_{cl}} \quad (98)$$

In that case we never leave the small n regime and this approximation remains valid even for large time as can be seen on Fig. 13.

6.2 Periodic Soliton Pulses

When time increases, the approximation $n \ll 1$ is not valid anymore and we must take into account the exact quantum Hamiltonian. In the regime $\hbar \ll x = n\hbar \ll 2s_{cl}$, we can still perform a WKB approximation. The previous discussion has shown that the semi classical wave-function is concentrated on the classical orbit of h^0 with energy $E = E_c + \hbar\kappa$, that is $\epsilon = \kappa$. We set:

$$p(x, t) = e^{-\frac{i}{\hbar}\kappa(2s_{cl} + \hbar)t} e^{-\frac{i}{\hbar}(W_0(x) + \hbar W_1(x))} b(x, t)$$

where $W_0(x)$ is given by Eq. (74), and $W_1(x)$ by Eq. (77) in which ϵ is replaced by its actual value κ . The only source of time dependence, at this level of approximation, arises from the transport equation of the amplitude. Let us define the local velocity $v(x)$ on the classical trajectory by:

$$v(x) = -\partial_\theta h^0(x, W_0'(x)) = \pm 2x \sqrt{\Omega^2 - x}$$

From this field, we obtain the Hamiltonian flow on the classical trajectory by solving the differential equation $dx/dt = v(x)$. Let us denote by $x(x_0, t)$ the solution of this equation which starts from x_0 at $t = 0$. Likewise, we may reverse the flow and define $x_0(x, t)$. It is convenient to introduce the function $u(x)$ such that $du/dx = -1/v(x)$. The solution of the flow is then:

$$u(x_0) = u(x) + t \quad (99)$$

For our problem, we have:

$$u(x) = - \int^x \frac{1}{2x\sqrt{\Omega^2 - x}} dx, \quad \text{or else} \quad x = \frac{\Omega^2}{\cosh^2 \Omega u}$$

The transport equation simply states the conservation of the local density $b^2(x, t)$:

$$\partial_t(b^2(x, t)) + \partial_x(b^2(x, t)v(x)) = 0$$

The evolution of this one dimensional conserved fluid is characterized by the invariance of b^2v along the flow:

$$b^2(x, t)v(x) = b^2(x_0(x, t), 0)v(x_0(x, t)) \equiv B_0^2(u(x) + t) \quad (100)$$

which simply results from the conservation law and the fact that the velocity field does not depend on time.

Then we have:

$$\bar{x}(t) = \int dx \frac{x}{[x^2(\Omega^2 - x)]^{1/2}} B_0(u(x) + t)^2 = \int du \frac{\Omega^2}{\cosh^2 \Omega u} B_0(u + t)^2 \quad (101)$$

If we assume that $B_0(u)^2$ is peaked around t_0 , say $B_0(u)^2 = \delta(u - t_0)$, we find:

$$\bar{x}(t) = \frac{\Omega^2}{\cosh^2 \Omega(t - t_0)} \quad (102)$$

which is just the classical expression. There is a simple way to evaluate the time t_0 . In fact there must be a regime where the small time formula and this semiclassical formula should agree. i.e.

$$\hbar \frac{2s_{cl}}{\Omega^2} \sinh^2 \Omega t \simeq \frac{\Omega^2}{\cosh^2 \Omega(t - t_0)}, \quad \text{or} \quad \hbar \frac{2s_{cl}}{4\Omega^2} e^{2\Omega t} \simeq 4\Omega^2 e^{2\Omega(t-t_0)} \quad (103)$$

and this gives the time t_0 :

$$t_0 = -\frac{1}{2\Omega} \log \frac{2s_{cl}}{16\Omega^4} \hbar \simeq -\frac{1}{2\Omega} \log \hbar + O(\hbar^0) \quad (104)$$

This reproduces well the position of the first peak. Its height is also well reproduced if instead of the crude approximation $B_0(u)^2 = \delta(u - t_0)$, we glue the wave functions given by the small time solution and the WKB solution at a gluing time t_g :

$$B_0(u + t_g)^2 \simeq K \frac{\sinh(\Omega u)}{\cosh(\Omega u)^3} \exp\left(-\frac{\Omega^2}{\bar{x}(t_g) \cosh(\Omega u)^2}\right)$$

where the normalization constant K is given by the condition:

$$\int_0^\infty B_0(u)^2 du = 1$$

and $\bar{x}(t_g)$ is the value of \bar{x} given by Eq. (97) taken at time $t = t_g$ (see Fig. 17). The height of the

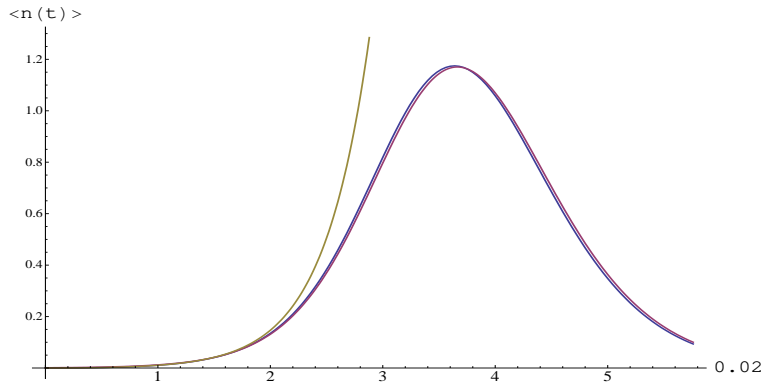


Figure 17: Time evolution of the mean oscillator energy $\bar{x}(t)$ for $\kappa = 1/\sqrt{2}$, $s_{cl} = 1$ and $\hbar = 1/300$. The blue line corresponds to the exact solution, the red one to the semiclassical solution and the yellow line to the small time solution.

first peak can be estimated from Eq. (101). The maximum is obtained when we have the largest overlap between $1/\cosh^2 \Omega u$ and $B_0(u + t)^2$. This happens with a very good approximation, for $t = t_0$ such that the maximum of $B_0(u + t_0)^2$ is at zero:

$$\sinh^2 \Omega(t_0 - t_g) = -\frac{1}{4} \left(1 - \frac{2\Omega}{\bar{x}(t_g)}\right) + \sqrt{\frac{1}{16} \left(1 - \frac{2\Omega}{\bar{x}(t_g)}\right)^2 + \frac{1}{2}}$$

The previous equation allows us also to discuss the freedom in the choice of the gluing point t_g . Indeed we expect that t_0 does not depend on t_g as long as t_g is restricted to a temporal domain where the short time solution and the semiclassical one overlap. If we plot t_0 as a function of t_g , we see that the curve we obtain develops a plateau, which means that the value of t_0 we obtain choosing t_g inside this plateau is independent of t_g .

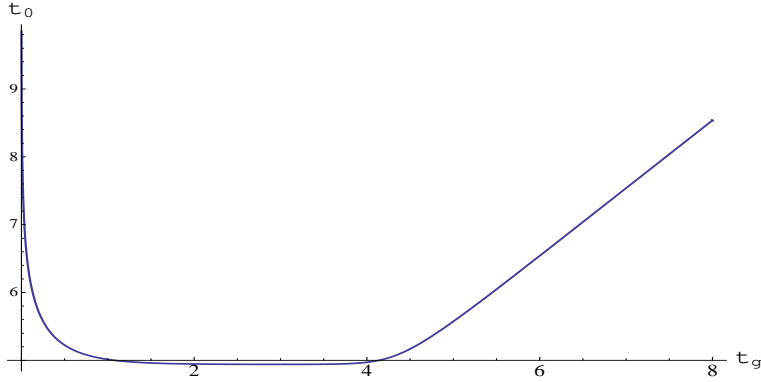


Figure 18: Time t_0 of the first pulse as a function of the gluing time t_g between the short time solution and the WKB solution. The existence of a plateau shows that gluing can be done in an unambiguous way. $\kappa = -1/\sqrt{2}$, $s_{cl} = 1$ and $\hbar = 10^{-4}$. We can recognize a plateau between $t_g = 1$ and $t_g = 4$.

Moreover, if we plot the value of t_0 at the plateau, as a function of $\log(\hbar)$, we recover with a very good accuracy the rough estimation of Eq. (104), see Fig. 19.

If we return to the *delta*-function approximation, it is clear that the situation reproduces itself after a time interval $2t_0$. Hence we can write:

$$\bar{x}(t) \simeq \sum_{k=-\infty}^{\infty} \frac{\Omega^2}{\cosh^2 \Omega(t - (2k + 1)t_0)} \simeq \Omega^2 \text{cn}^2[\Omega(t - t_0)|k^2]$$

where cn is a Jacobi elliptic function of modulus k^2 given approximately by:

$$k^2 \simeq 1 - \frac{2\hbar s_{cl}}{\Omega^4}$$

When $\kappa = 0$, this is Bonifacio and Preparata's result [9]. Clearly, it remains a challenge to account for the lack of exact periodicity in the pulse sequence, using the time-dependent approach. In this perspective, returning to the integrable structure may be interesting in order to obtain an effective model around the critical point in terms of particle-hole excitations of Bethe pseudo-particles.

7 Conclusion

Let us emphasize the main results of this work. First, the Jaynes-Cummings model exhibits, in a large region of its parameter space, an unstable fixed point which corresponds to the focus-focus

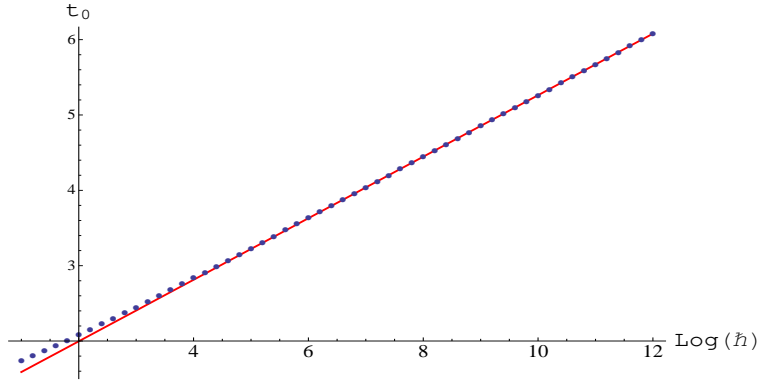


Figure 19: Time t_0 of the first pulse as a function of \hbar . The blue points are obtained by looking at the value of t_0 at the plateau. The red line corresponds to the Eq. (104). $\kappa = -1/\sqrt{2}$, $s_{cl} = 1$.

singularity of an integrable system with two degrees of freedom. As a result, there is a classical monodromy when one considers a loop which encircles the critical value in the (H_0, H_1) plane. At the quantum level, this phenomenon is manifested by a dislocation in the joint spectrum of H_0 and H_1 . We have then analyzed the eigen-subspace of H_1 which corresponds to the critical point. The associated reduced phase-space is a sphere. We have shown how to perform a semi-classical analysis using the convenient but singular coordinates (x, θ) on this sphere. The main result here is that when the classical orbit crosses either the north or the south pole, where the longitude θ is not well defined, the action integral associated to the subprincipal symbol jumps by $\pm\pi$, and this is compensated by a simultaneous jump in the Maslov index. Most of the spectrum is well described by usual Bohr-Sommerfeld quantization rules, at the exception of typically $|\log \hbar|$ eigenstates in the vicinity of the critical energy, for which special Bohr-Sommerfeld rules have been obtained. Remarkably, the classical unstable equilibrium state, where the spin component s^z is maximal and the oscillator is in its ground-state, has most of its weight on the subspace spanned by these singular semi-classical states. This fact explains rather well the three time scales observed in the evolution of the mean energy of the oscillator. At short time, this energy grows exponentially, reflecting the classical instability of the initial condition. At intermediate times, the energy of the oscillator exhibits a periodic sequence of pulses, which are well described by the classical motion along the pinched torus containing the unstable point. Finally, the delicate pattern of energy levels, which are not exactly equidistant, governs the aperiodic behavior observed for longer time scales.

This work leaves many unsolved questions. One of them is to develop a detailed analytical description of the long time behavior. This should a priori be possible because, as we have seen, the initial state is a linear superposition of only a small number of energy eigenstates, for which the singular WKB analysis developed here provides an accurate modeling. Another interesting direction is the extension to several spins, which is physically relevant to the dynamics of cold

atom systems after a fast sweep through a Feshbach resonance. It would be interesting to discuss if the notion of monodromy can be generalized with more than two degrees of freedom. Finally, it remains to see whether the qualitative features of the time evolution starting from the unstable state remain valid for an arbitrary number of spins, as may be conjectured from the structure of the quadratic normal form in the vicinity of the singularity.

8 Acknowledgements

One of us (B.D.) would like to thank Yshai Avishai for many stimulating discussions on out of equilibrium dynamics of cold atom systems and for an initial collaboration on this project. We have also benefited a lot from many extended discussions with Thierry Paul on various aspects of semi-classical quantization. Finally, we wish to thank Yves Colin de Verdière and Laurent Charles for sharing their knowledge with us. B.D. was supported in part by the ANR Program QPPRJCCQ, ANR-06BLAN-0218-01, O.B. was partially supported by the European Network ENIGMA, MRTN-CT-2004-5652 and L.G. was supported by a grant of the ANR Program GIMP, ANR-05-BLAN-0029-01.

References

- [1] E. Jaynes, F. Cummings, *Comparison of quantum and semiclassical radiation theories with application to the beam maser*, Proc. IEEE **51**, 89 (1963).
- [2] J. Ackerhalt, K. Rzazewski, *Heisenberg-picture operator perturbation theory*. Phys. Rev. A, **12**, 2549 (1975).
- [3] N. Narozhny, J. Sanchez-Mondragon, J. Eberly, *Coherence versus incoherence: Collapse and revival in a simple quantum model*. Phys. Rev. A **23**, 236 (1981).
- [4] G. Rempe, H. Walther, and N. Klein, *Observation of quantum collapse and revival in a one-atom maser*, Phys. Rev. Lett. **58**, 353 (1987).
- [5] M. Brune, F. Schmidt-Kaler, A. Maali, J. Dreyer, E. Hagley, J. M. Raimond, and S. Haroche, *Quantum Rabi oscillation: A direct test of field quantization in a cavity*, Phys. Rev. Lett. **76**, 1800 (1996).
- [6] J. Gea-Banacloche, *Atom and field-state evolution in the Jaynes-Cummings model for large initial fields*, Phys. Rev. A **44**, 5913 (1991).
- [7] M. Brune, E. Hagley, J. Dreyer, X. Maître, A. Maali, C. Wunderlich, J. M. Raimond, and S. Haroche, *Observing the progressive decoherence of the “meter” in a quantum measurement*, Phys. Rev. Lett. **77**, 4887 (1996).
- [8] R. H. Dicke, *Coherence in spontaneous radiation processes*, Phys. Rev. **93**, 99 (1954).
- [9] R. Bonifacio and R. Preparata, *Coherent spontaneous emission*, Phys. Rev. A **2**, 336 (1970).
- [10] M. Greiner, C. A. Regal, and D. S. Jin, *Emergence of a molecular Bose-Einstein condensate from a Fermi gas*, Nature **426**, 537 (2003).
- [11] T. Bourdel, L. Khaykovich, J. Cubizolles, J. Zhang, F. Chevy, M. Teichmann, L. Tarruell, S. J. Kokkelmans, and C. Salomon, *Experimental study of the BEC-BCS crossover region in lithium 6*, Phys. Rev. Lett. **93**, 050401 (2004).
- [12] M.W. Zwierlein, C. A. Stan, C. H. Schunck, S. M. F. Raupach, A. J. Kerman, and W. Ketterle, *Condensation of pairs of fermionic atoms near a Feshbach resonance*, Phys. Rev. Lett. **92**, 120403 (2004).
- [13] R. A. Barankov and L. S. Levitov, *Atom-molecule coexistence and collective dynamics near a Feshbach resonance of cold fermions*, Phys. Rev. Lett. **93**, 130403.

- [14] E. Yuzbashyan, V. Kuznetsov, B. Altshuler, *Integrable dynamics of coupled Fermi-Bose condensates*, Phys. Rev. B **72**, 144524 (2005).
- [15] M. Gaudin, *La fonction d'onde de Bethe*, chapter 13, Masson, Paris (1983).
- [16] Y. Colin de Verdière and B. Parisse, *Equilibre instable en régime semi-classique: I-Concentration microlocale*, Commun. PDE, **19**, 1535, (1994).
- [17] Y. Colin de Verdière and B. Parisse, *Equilibre instable en régime semi-classique: II-Conditions de Bohr-Sommerfeld*, Annales de l'I. H. P., **61**, 347, (1994).
- [18] R. Brummelhuis, T. Paul, and A. Uribe, *Spectral estimates around a critical level*, Duke Math. J. **78**, 477, (1995).
- [19] M. S. Child *Quantum states in a champagne bottle*, J. Phys. A **31**, 657, (1998).
- [20] Y. Colin de Verdière and B. Parisse, *Singular Bohr-Sommerfeld rules*, Comm. Math. Phys. **205**, 459, (1999).
- [21] J. J. Duistermat, *On global action-angle coordinates*, Comm. Pure Appl. Math. **33**, 687, (1980).
- [22] L. Bates, *Monodromy in the champagne bottle*, J. Appl. Math. Phys. **42**, 837, (1991).
- [23] S. Vũ Ngọc, *Quantum monodromy in integrable systems*, Comm. Math. Phys. **203**, 465, (1999).
- [24] D. A. Sadovskii and B. I. Zhilinskii, *Quantum monodromy, its generalizations and molecular manifestations*, Mol. Phys. **104**, 2595, (2006).
- [25] M. Zou, *Monodromy in two degrees of freedom integrable systems*, J. Geom. Phys. **10**, 37, (1992).
- [26] N. T. Zung, *A note on focus-focus singularities*, Diff. Geom. Appl. **7**, 123 (1997).
- [27] R. Cushman and J. J. Duistermat, *Non-Hamiltonian monodromy*, J. Diff. Eqs. **172**, 42, (2001).
- [28] S. Vũ Ngọc, *Bohr-Sommerfeld conditions for integrable systems with critical manifold of focus-focus type*, Comm. Pure Appl. Math. **53**, 143, (2000).
- [29] M. Bellon, M. Talon, *Spectrum of the quantum Neumann model*. Phys.Lett. **A337**, 360, (2005). *The quantum Neumann model: asymptotic analysis*. Phys. Lett. **A 351**, 283, (2006). *The quantum Neumann model: refined semiclassical results*. Phys.Lett. **A356**, 110, (2006).

- [30] A. Faribault, P. Calabrese and J. S. Caux, *Quantum quenches from integrability: the fermionic pairing model*, J. Stat. Mech. (2009), P03018.
- [31] F. A. Berezin, *General concept of quantization*, Comm. Math. Phys. **40**, 153, (1975).
- [32] L. Charles, *Symbolic calculus for Toeplitz operators with half-form*, Journ. Symplec. Geom. **4**, 171, (2006).
- [33] J. J. Duistermaat, *Oscillatory integrals, Lagrange immersions, and unfolding of singularities*, Comm. Pure Appl. Math. **27**, 207, (1974).
- [34] J. Keeling, *Quantum corrections to the semiclassical collective dynamics in the Tavis-Cummings model*, arXiv:0901.4245
- [35] C. Leichtle, I. Sh. Averbukh, and W. P. Schleich, *Generic structure of multilevel quantum beats*, Phys. Rev. Lett. **77**, 3999, (1996).
- [36] A. Micheli, D. Jaksch, J. I. Cirac, and P. Zoller, *Many-particle entanglement in two-component Bose-Einstein condensates*, Phys. Rev. A **67**, 013607, (2003).
- [37] E. Boukobza, M. Chuchem, D. Cohen, and A. Vardi, *Phase-diffusion dynamics in weakly coupled Bose-Einstein condensates*, arXiv:0812.1204